Article

Suppression of proteolipid protein rescues Pelizaeus–Merzbacher disease

Matthew S. Elitt[1], Lilianne Barbar[1], H. Elizabeth Shick[1], Berit E. Powers[2], Yuka Maeno-Hikichi[1], Mayur Madhavan[1], Kevin C. Allan[1], Baraa S. Nawash[1], Artur S. Gevorgyan[1], Stevephen Hung[1], Zachary S. Nevin[1], Hannah E. Olsen[1], Midori Hitomi[3], Daniela M. Schlatzer[4], Hien T. Zhao[2], Adam Swayze[2], David F. LePage[1], Weihong Jiang[1], Ronald A. Conlon[1], Frank Rigo[2] & Paul J. Tesar[1]✉

Mutations in *PLP1*, the gene that encodes proteolipid protein (PLP), result in failure of myelination and neurological dysfunction in the X-chromosome-linked leukodystrophy Pelizaeus–Merzbacher disease (PMD)[1,2]. Most *PLP1* mutations, including point mutations and supernumerary copy variants, lead to severe and fatal disease. Patients who lack *PLP1* expression, and *Plp1*-null mice, can display comparatively mild phenotypes, suggesting that *PLP1* suppression might provide a general therapeutic strategy for PMD[1,3–5]. Here we show, using CRISPR–Cas9 to suppress *Plp1* expression in the *jimpy* (*Plp1^{jp}*) point-mutation mouse model of severe PMD, increased myelination and restored nerve conduction velocity, motor function and lifespan of the mice to wild-type levels. To evaluate the translational potential of this strategy, we identified antisense oligonucleotides that stably decrease the levels of *Plp1* mRNA and PLP protein throughout the neuraxis in vivo. Administration of a single dose of *Plp1*-targeting antisense oligonucleotides in postnatal *jimpy* mice fully restored oligodendrocyte numbers, increased myelination, improved motor performance, normalized respiratory function and extended lifespan up to an eight-month end point. These results suggest that *PLP1* suppression could be developed as a treatment for PMD in humans. More broadly, we demonstrate that oligonucleotide-based therapeutic agents can be delivered to oligodendrocytes in vivo to modulate neurological function and lifespan, establishing a new pharmaceutical modality for myelin disorders.

PMD (Online Mendelian Inheritance in Man (OMIM) ID: 312080) is a fatal, X-linked leukodystrophy characterized by extensive loss of myelinating oligodendrocytes in the central nervous system (CNS). Mutations in the *PLP1* gene, which encodes the highly conserved four-transmembrane-domain oligodendrocyte protein PLP, cause PMD[1,2]. Symptoms typically present at birth or in childhood, and include a constellation of nystagmus, spasticity, hypotonia and cognitive dysfunction, leading to early death, often before adulthood. Preclinical efforts to extend lifespan have had only limited success, and no therapy has shown efficacy in patients[6–13].

Most patients with PMD have *PLP1*-duplication mutations, which cause overexpression of otherwise normal PLP protein[1,2]. However, hundreds of distinct PMD-causative point mutations, which result in abnormal PLP protein, have also been identified. Notably, rare patients who lack *PLP1* expression display symptoms that are delayed and milder compared with those with more severe duplications or point mutations[3–5]. These *PLP1*-null patients can live for 40–60 years, do not develop spastic paraparesis until the second or third decade of life, and maintain intact cognition until the third or fourth decade of

life (Supplementary Table 1), possibly owing to a lack of cellular stress responses and oligodendrocyte death triggered by excess or abnormal PLP[1,2,12,14,15].

This clinical landscape suggests several opportunities for therapeutic development. Specifically, reducing *PLP1* expression to normal levels in patients with gene duplications would be expected to be curative. More broadly, the milder presentation of patients lacking *PLP1* implies a wide therapeutic window for titrating *PLP1* expression, which could be leveraged to restore functional oligodendrocytes in patients with point mutations that generate abnormal PLP. Here we demonstrate therapeutic *Plp1* suppression using germline- and postnatal-based approaches in a mouse model of PMD that expresses abnormal PLP.

Germline suppression of *Plp1* in PMD mice

To test whether *Plp1* suppression provides a generalizable therapeutic approach for PMD, we used the *jimpy* (*Plp1^{jp}*) mouse model of PMD, which expresses abnormal PLP and recapitulates the cellular, molecular and neurologic features seen in severe PMD. We targeted *Plp1* with

[1]Department of Genetics and Genome Sciences, Case Western Reserve University School of Medicine, Cleveland, OH, USA. [2]Ionis Pharmaceuticals, Carlsbad, CA, USA. [3]Lerner Research Institute, Cleveland Clinic, Cleveland, OH, USA. [4]Case Center for Proteomics and Bioinformatics, Department of Medicine, Case Western Reserve University School of Medicine, Cleveland, OH, USA. ✉e-mail: paul.tesar@case.edu

Article

CRISPR[16,17], using single guide RNAs (sgRNAs) with high on-target, germline cutting efficiency (Supplementary Table 2), to generate a CRISPR-modified *jimpy* (CR-*impy*) founder with a complex deletion in *Plp1* (Fig. 1a, Extended Data Fig. 1a–c). Before subsequent analyses, rare off-target mutations were eliminated by back-crossing (Extended Data Fig. 1b, d, e).

Whereas *jimpy* mice showed severe tremor, ataxia, seizures (lasting more than 30 s) and death by the third postnatal week, CR-*impy* mice exhibited a 21-fold increase in lifespan (mean survival 489 and 23 days for CR-*impy* and *jimpy* mice, respectively) with no evidence of tremor, ataxia or seizures up to the terminal end point of 18 months of age (Fig. 1b, Supplementary Data 1, Supplementary Videos 1, 2). The level of *Plp1* transcript in CR-*impy* mice was reduced by 61–74% relative to wild type in multiple CNS regions at 6 months of age (Extended Data Fig. 2a), with undetectable levels of PLP protein (Supplementary Table 3).

To explore the effects of germline *Plp1* suppression on cellular pathology, we assessed markers of oligodendrocyte lineage and neuroinflammation. The mature myelin marker myelin basic protein (MBP) was grossly and stably restored to near wild-type levels throughout the neuraxis in CR-*impy* mice (Fig. 1c). In contrast to the almost complete absence of *Mbp* expression in *jimpy* mice, CR-*impy* mice demonstrated substantially increased transcript (83–91% of wild type at 6 months of age) and protein (40–95% and 114–130% of wild type at 3 weeks and 6 months of age, respectively) in multiple CNS regions (Extended Data Fig. 2b–d, Supplementary Data 2a, b, 3–5). Quantification of myelin regulatory factor (MyRF)-positive oligodendrocytes showed their complete restoration throughout multiple CNS regions in CR-*impy* mice (94–117% and 89–126% of wild type at 3 weeks and 6 months of age, respectively), in contrast to their depletion in *jimpy* mice (36–59% of wild type at 3 weeks of age) (Fig. 1d, e, Supplementary Data 3–5). The glial lineage marker SOX10, which is expressed by oligodendrocytes and oligodendrocyte progenitor cells (OPCs), showed no differences across these genotypes (Fig. 1d, e, Supplementary Data 3–5). CR-*impy* mice showed minimal evidence of astrogliosis or microglial activation up to 6 months of age, in contrast to elevated neuroinflammatory markers in *jimpy* mice[18] (Extended Data Fig. 3a–d, Supplementary Data 3–5).

To investigate *Plp1* suppression in oligodendrocytes isolated from cell-extrinsic developmental or inflammatory cues, we generated and characterized induced pluripotent stem cell lines (Extended Data Fig. 4a, b), which were differentiated to oligodendrocytes in vitro. Notably, CR-*impy* lines showed cell-type-specific rescue in oligodendrocyte number and arborized morphology relative to *jimpy* lines (Extended Data Fig. 4c–g). Collectively, these data confirm that *Plp1* suppression has a cell-intrinsic effect on oligodendrocytes that is sufficient to rescue *jimpy* cellular phenotypes.

To assess the effect of germline *Plp1* suppression on myelination, we quantified electron micrograph data. In contrast to nearly absent myelination in *jimpy* mice, CR-*impy* mice showed a marked increase in myelinated axons throughout the neuraxis, reaching nearly 50% of that in wild-type mice by 3 weeks of age, with stability up to 18 months of age (Fig. 1f–h). Myelin sheaths in CR-*impy* mice showed incomplete compaction compared with those in the wild-type mice, consistent with the role of PLP in myelin ultrastructure[5,19] (Fig. 1f, g). To determine whether myelin in CR-*impy* mice was functional, we measured compound action potential speed in the optic nerve. At 3 weeks of age, we found a significant increase in conduction velocity in CR-*impy* mice relative to *jimpy* mice (Fig. 1i) (reaching approximately 55% of that in the wild type), which was well-correlated with the level of myelination in CR-*impy* mice (approximately 35% of the wild-type level) (Fig. 1j). Notably, CR-*impy* and wild-type mice showed similar conduction velocities at 6 months of age (Fig. 1i).

To determine whether restored myelin altered complex motor function, we used longitudinal open-field and rotarod testing. Overall locomotion was decreased in *jimpy* mice, but similar between CR-*impy* and wild-type mice across all time points (Fig. 1k). Rotarod testing revealed that CR-*impy* mice showed similar performance to wild-type mice up to 6 months of age, whereas *jimpy* mice exhibited significant impairment. At 18 months of age, the CR-*impy* mice displayed slightly reduced performance (Fig. 1l), potentially reflecting late-onset neuronal phenotypes[4]. Together, these results establish that germline suppression of *Plp1* restores oligodendrocytes, functional myelin and lifespan in *jimpy* mice.

In vivo suppression of oligodendrocyte transcripts

After validating *Plp1* as a therapeutic target for PMD using germline suppression, we pursued a clinically translatable strategy for in vivo, postnatal *Plp1* suppression using newer-generation antisense oligonucleotides (ASOs). These ASOs, distinguished by their highly efficient modulation of target transcripts in the CNS with multi-month in vivo half-lives, underlie several therapies for fatal neuronal-based disorders[20–22]; however their ability to target the oligodendrocyte lineage in vivo was unknown. To establish their therapeutic potential for this lineage, we administered well-characterized ASOs targeting *Hdac2* to adult wild-type mice by intracerebroventricular (ICV) injection. HDAC2 protein is localized to the nucleus and enables clear visualization of target suppression; ICV injection of ASOs targeting *Hdac2* resulted in a substantial reduction of HDAC2 levels in OPCs and oligodendrocytes (Fig. 2a, b). Next we identified two independent ASOs targeting the fifth intron (ASO*Plp1*.a) and 3′-untranslated region (UTR) (ASO*Plp1*.b) of *Plp1* (Fig. 2c), along with a non-targeting ASO control (ASOctr), which we administered to wild-type mice. These ASOs showed dose-dependent suppression of *Plp1* transcript (up to 90% and 98% suppression in neonatal and adult wild-type mice, respectively) and PLP protein (up to 63% in neonatal wild-type mice) in multiple CNS regions (Fig. 2d–g, Extended Data Fig. 5a). They also showed widespread distribution across the neuraxis, did not exhibit off-target effects on non-*Plp1* transcripts, did not activate glial cells and did not alter levels of MBP protein in wild-type mice (Extended Data Figs. 5b–h, 6a, b, 7a, Supplementary Data 7a).

## Postnatal *Plp1* suppression in PMD mice

We evaluated the therapeutic effect of *Plp1*-targeting ASOs on the severe *jimpy* phenotype using a single ICV injection at birth (Fig. 3a). *Jimpy* mice injected with ASO*Plp1*.a or ASO*Plp1*.b exhibited increases in lifespan of approximately 12-fold and 11-fold, respectively, compared with *jimpy* mice injected with ASOctr (mean survival of 20 (ASOctr), 239 (ASO*Plp1*.a) and 217 days (ASO*Plp1*.b)) up to a predetermined terminal end point of 8 months of age (Fig. 3b, Supplementary Data 6, Supplementary Videos 3, 4).

MBP expression was grossly increased in *jimpy* mice treated with ASO*Plp1*.a or ASO*Plp1*.b relative to those treated with ASOctr up to eight months of age, without additional ASO dosing (Fig. 3c, d). Levels of *Mbp* transcript and MBP protein were significantly increased across the neuraxis in *jimpy* mice treated with ASO*Plp1*.a or ASO*Plp1*.b compared with those treated with ASOctr (up to a 39-fold increase in MBP protein), along with a concomitant reduction in apoptotic cells (Extended Data Fig. 7b–e, Supplementary Data 7b, 8–10). MyRF-positive oligodendrocytes were substantially depleted in *jimpy* mice treated with ASOctr but were restored throughout the neuraxis at 3 weeks of age in *jimpy* mice treated with ASO*Plp1*.a or ASO*Plp1*.b (81–101% of the level in wild-type mice treated with ASOctr) (Fig. 3e, Supplementary Data 8–10). These trends were further validated by examining OLIG2 and CC1 double-positive oligodendrocytes (Extended Data Fig. 7f, Supplementary Data 11–13). There were similar levels of SOX10- and OLIG2-positive oligodendrocyte lineage cells across groups (Fig. 3f, Extended Data Fig. 7g, Supplementary Data 8–13). Levels of PDGFRα and OLIG2 double-positive OPCs were similar in wild-type mice treated with ASOctr and in *jimpy* mice treated with ASO*Plp1*.a and ASO*Plp1*.b,
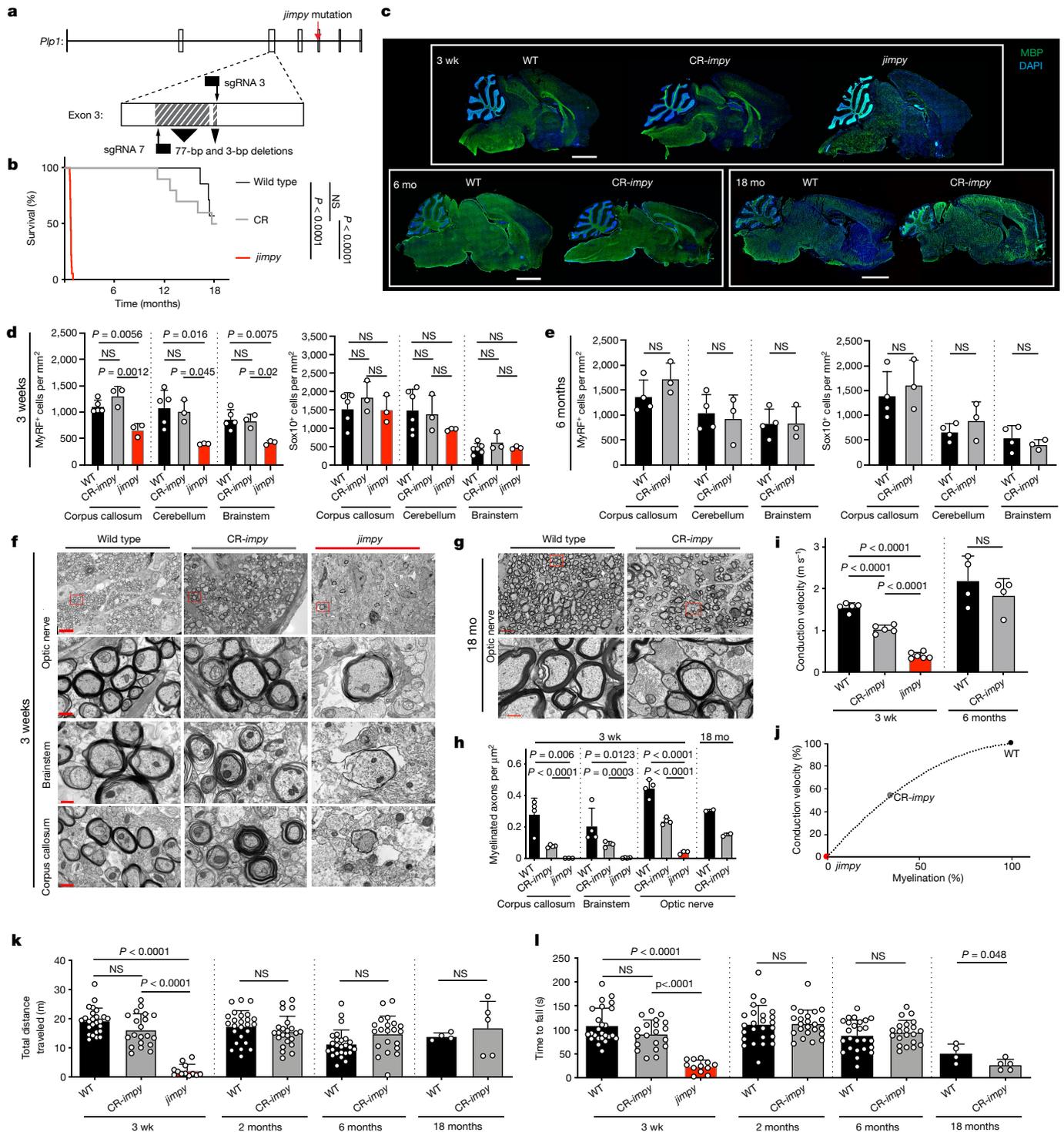
Fig. 1 | Germline *Plp1* suppression in *jimpy* rescues lifespan and restores functional myelin. a, Schematic of CRISPR *Plp1* targeting in *jimpy*. Black arrowheads indicate predicted sgRNA cutting sites. Hashed boxes show the CR-*impy* 80-base pair (bp) complex deletion (Extended Data Fig. 1a). **b**, Kaplan–Meier plot comparing lifespans between genotypes. *n* = 25 (wild type (WT)), 23 (CR-*impy*) and 18 (*jimpy*) mice. *P* values calculated using log-rank test. **c**, Immunohistochemistry of whole-brain sagittal sections of 3-week-old (wk), 6-month-old (mo) and 18 month-old wild-type (WT), CR-*impy* and *jimpy* mice showing MBP (green) and nuclei (DAPI, blue). Scale bars, 2 mm. **d**, **e**, Quantification of MyRF+ and SOX10+ cells at three weeks (**d**) and six months (**e**) of age. *n* = 3–6 mice. Representative source images are presented in Supplementary Data 3–5. **f**, **g**, Electron micrographs showing myelination at 3 weeks (**f**) and 18 months (**g**) of age. Higher magnification of the red boxed area shown in the next row. Scale bars, 5 μm (top row) and 0.5 μm (other rows).

h, Quantification of myelinated axons at 3 weeks (*n* = 3–4 mice) and 18 months (*n* = 2 mice) of age. *P*-values calculated with unpaired, two-sided *t*-tests. **i**, Optic nerve conduction velocities at 3 weeks (*n* = 5–6 mice) and 6 months (*n* = 4 mice). **j**, Polynomial trend line illustrating conduction velocity versus brain myelination in CR-*impy* relative to minimum–maximum scaling of values from *jimpy* and wild-type mice. Data from three-week time point of **h** and **i**, with same *n*. **k**, **l**, Accelerating rotarod (**k**) or open-field (**l**) performance. *n* = 25 (WT), 20 (CR-*impy*) and 12 (*jimpy*) mice at 3 weeks of age; *n* = 25 (WT), 23 (CR-*impy*) mice at 2 months of age; *n* = 25 (WT), 21 (CR-*impy*) mice at 6 months of age; and *n* = 4 (WT), 5 (CR-*impy*) mice at 18 months of age. Biological replicates (individual mice) indicated by open circles. Data are mean ± s.d. *P* values calculated using one-way analysis of variance (ANOVA) with Tukey's correction at three weeks or two-way, unpaired two-sided *t*-test at later time points, except where indicated. *P* values shown for *P* < 0.1, otherwise not significant (NS).
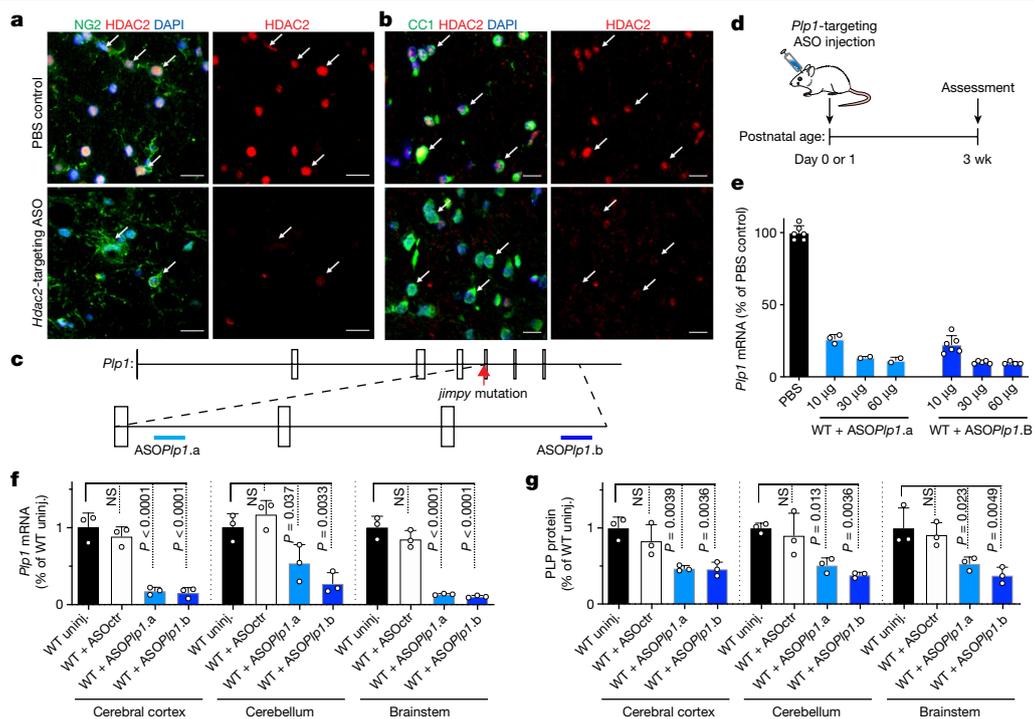
Fig. 2 | Efficient ASO-mediated transcript suppression in OPCs and oligodendrocytes in vivo. a, b, Immunostaining of HDAC2^{+} (red) and NG2^{+} OPCs (green; arrows) in the spinal cord (**a**) or CC1^{+} oligodendrocytes (green; arrows) in the corpus callosum (**b**) from eight-week-old wild-type mice injected with PBS control or *Hdac2*-targeting ASO, two weeks after injection. Scale bars, 20 μm. **c,** Depiction of *Plp1* pre-mRNA, showing the approximate binding locations of ASO*Plp1*.a and ASO*Plp1*.b in intron 5 and the 3' UTR, respectively. **d,** Schematic of the design of ASO experiments in this figure. **e,** Quantitative PCR with reverse transcription (RT–qPCR) data showing wild-type *Plp1* transcript levels in the spinal cord, 3 weeks after injection with the indicated

ASO doses (10 μg, 30 μg or 60 μg) or PBS controls at postnatal day 1 (*n* = 2–6 mice). **f, g,** RT–qPCR data showing the levels of *Plp1* transcript (**f**) and western blot data showing the levels of PLP protein (**g**), 3 weeks after ASO injection (30 μg dose) at birth in wild-type mice (*n* = 3 mice). Uninj., uninjected. Individual data points represent the mean value of four technical replicates for each biological replicate (**e, f**) or independent biological replicates (**g**). Biological replicates (individual mice) indicated by open circles. Data are mean ± s.d. *P* values calculated using one-way ANOVA with Dunnett's correction. *P* values shown for *P* < 0.1, otherwise not significant. See Supplementary Data 4 for full western blot source images.

but were increased in *jimpy* mice treated with ASOctr (Extended Data Fig. 7h, Supplementary Data 11–13), suggesting a *jimpy*-specific compensatory increase in progenitors[23]. Myelinated axons were significantly increased throughout the neuraxis in *jimpy* mice treated with ASO*Plp1*.a or ASO*Plp1*.b relative to those treated with ASOctr at 3 weeks of age (approximately 5–6-fold and 12–15-fold higher in the corpus callosum and brainstem, respectively) (Fig. 3g, h). Although oligodendrocyte numbers were fully restored, myelination in these mice was only about 10% of the level in wild-type mice treated with ASOctr at 3 weeks of age and persisted up to the 8-month end point, albeit with less compaction (Fig. 3g, h, Extended Data Fig. 8a, b).

Notably, *jimpy* mice treated with ASO*Plp1*.a or ASO*Plp1*.b showed only mild *jimpy* phenotypes, including markedly reduced tremor and occasional short-duration seizures (less than 15 s), and appeared outwardly normal otherwise, including in the ability to breed (Supplementary Data 6). Although rotarod performance of *jimpy* mice was only variably and partially improved with ASO*Plp1*.a or ASO*Plp1*.b treatment (to a maximum of 36% of wild-type performance), overall locomotion was restored to wild-type levels across multiple time points (Fig. 4a, b). To assess whether myelin might contribute to these functional improvements, we measured compound action potential speed in the optic nerve. At three weeks of age, we found a modest but significant increase in conduction velocity in *jimpy* mice treated with ASO*Plp1*.b versus ASOctr (Fig. 4c), representing about 17% of the level in wild-type mice treated with ASOctr; this result corresponds directly with the level of myelination relative to the wild-type control mice (about 10%) (Fig. 4d). Together, these data demonstrate that a single postnatal administration of *Plp1*-targeting ASOs in *jimpy* mice elicits a sustained reduction in *Plp1*

expression that restores oligodendrocytes and increases functional myelin, with improvements in motor performance and lifespan.

Respiratory distress and dysfunction has been associated with premature death in animal models of PMD and in patients with the disease[24–27], which is notable given the marked increase in survival of *jimpy* mice treated with ASO*Plp1*.a or ASO*Plp1*.b in light of the relatively modest increases in myelin globally, with the highest levels consistently observed in the brainstem (Fig. 3g, h, Extended Data 7b, c). Notably, brainstem respiratory control centres alter breathing patterns in response to physiological derangements seen during hypoxia or hypercapnia. Seizures, as observed in *jimpy* mice from around the third postnatal week, can trigger such derangements (Fig. 4e) and, when coupled with a reduced capacity to achieve homeostasis, could be lethal.

To investigate whether respiratory function is a therapeutic component of *Plp1*-targeting ASOs, we used plethysmography to measure minute ventilation in normal air, hypercapnic (5% CO_2) and hypoxic (10.5% O_2) conditions (Supplementary Data 14). When transitioned from normal air to either hypercapnic or hypoxic environments, *jimpy* mice treated with ASOctr exhibited high variability in minute ventilation, indicative of dysfunctional respiratory control (Fig. 4f), whereas those treated with ASO*Plp1*.b showed less variability and responses more similar to those of wild-type control mice (Fig. 4f–j). Specifically, *jimpy* mice treated with ASOctr showed weak compensatory decreases in minute ventilation when exposed to hypercapnic conditions relative to wild-type mice treated with ASOctr, which were restored in *jimpy* mice treated with ASO*Plp1*.b (Fig. 4g, h). During early transition to hypoxia, wild-type mice treated with ASOctr and *jimpy* mice treated
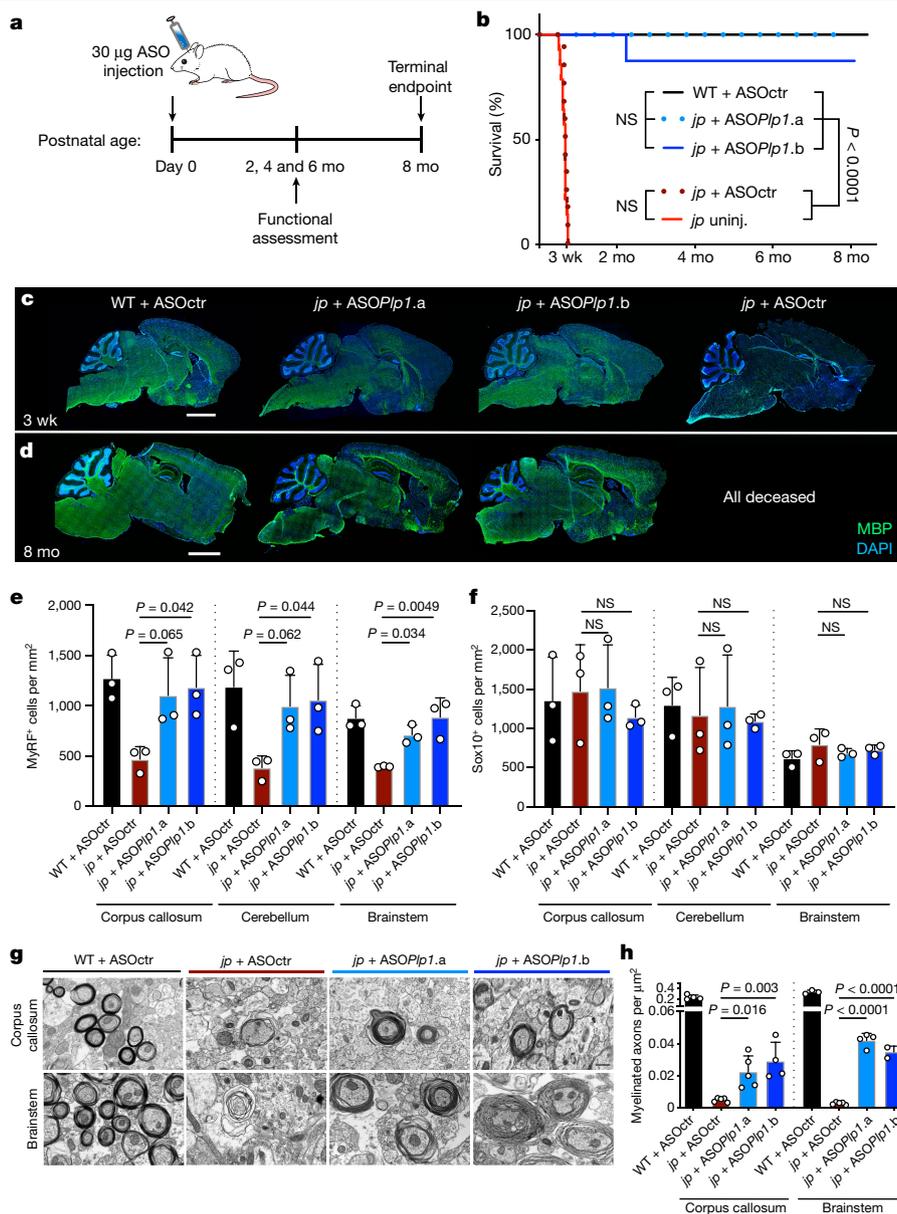
Fig. 3 | Postnatal delivery of *Plp1*-targeted ASOs rescues lifespan and oligodendrocytes with partial restoration of myelin in *jimpy* mice.
a, Schematic of ASO experimental design used in Figs. 3, 4. **b**, Kaplan–Meier plot showing the lifespan of contemporaneous wild-type mice treated with ASOctr (*n* = 12) and *jimpy* (*jp*) mice uninjected (*n* = 14) or injected with ASOctr, ASO*Plp1*.a (*n* = 5) or ASO*Plp1*.b (*n* = 5). *P* values calculated using the log-rank test. See Supplementary Data 6 for source metadata. **c**, **d**, Immunohistochemical images of 3-week-old (**c**) and 8-month-old (**d**) whole-brain sagittal sections showing MBP (green) and DAPI (blue) staining. Scale bars, 2 mm. See Supplementary Data 8–10 for higher magnification. **e**, **f**, Quantification of MyRF+ oligodendrocytes (**e**) and SOX10+ glial lineage cells (**f**) at 3 weeks of age (*n* = 3 mice). For representative source images, see Supplementary Data 8–10. **g**, **h**, Electron micrographs (**g**) and quantification (**h**) of myelinated axons at 3 weeks of age (*n* = 3–5 mice). Scale bar, 0.5 μm. Biological replicates (individual mice) indicated by open circles. Data are mean ± s.d. *P* values calculated using one-way ANOVA with Dunnett's correction, except where indicated. *P* values shown for *P* < 0.1, otherwise not significant.

with ASO*Plp1*.b demonstrated similar compensatory increases in minute ventilation, whereas *jimpy* mice treated with ASOctr showed a blunted response (Fig. 4g, i). In extended hypoxia, *jimpy* mice treated with ASOctr showed an exaggerated decrease in minute ventilation relative to wild-type controls, which was restored when they were treated with ASO*Plp1*.b (Fig. 4j). Of note, during this hypoxic challenge, 38% of *jimpy* mice treated with ASOctr died spontaneously, whereas 100% of those treated with ASO*Plp1*.b and wild-type mice treated with ASOctr survived (Fig. 4k). Together, these results suggest that dysregulated control of respiration is a component of the *jimpy* phenotype and potentially underlies the premature mortality that occurs coincident with the onset of seizures, and can be partially rescued by suppression of *Plp1*.

Discussion

In summary, we have validated a clinically feasible therapeutic strategy for PMD using a mutation-agnostic approach based on suppression of PLP. We demonstrate that suppression of *Plp1* expression using CRISPR–Cas9 in the germline or postnatal ASO results in rescue of major PMD phenotypes in a mouse model of severe PMD. Furthermore, we establish that oligonucleotide-based drugs, delivered postnatally, can modulate a disease target in oligodendrocytes and restore both functional myelin and lifespan in mice with a fatal genetic disorder.

This study provides foundational data for the development of clinically relevant ASO technology to achieve postnatal reduction of *PLP1*.
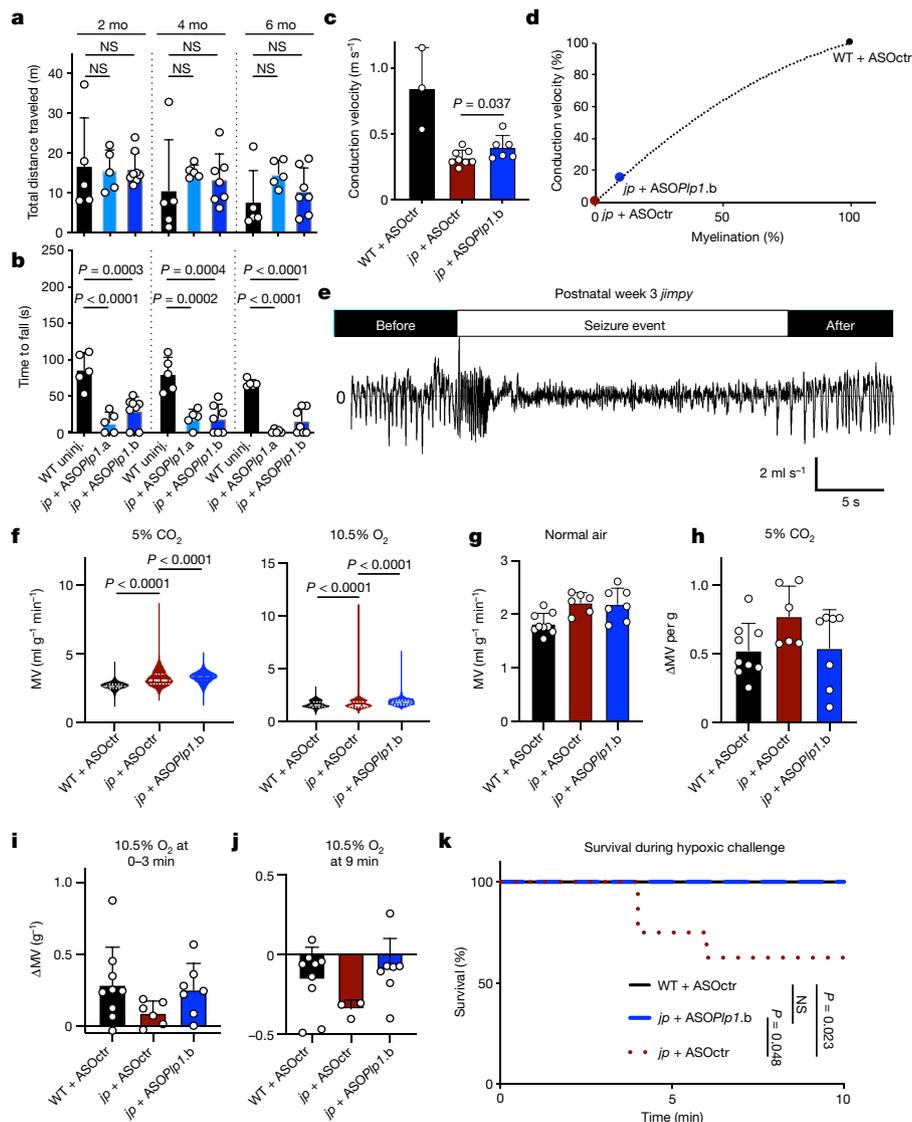
Fig. 4 | ASO-mediated *Plp1* suppression in *jimpy* leads to functional myelin, improved control of respiratory function and prevention of hypoxia-induced mortality. a, **b**, Performance in open-field testing (**a**) and accelerating rotarod (**b**) (*n* = 5–8 mice). Raw data is presented in Supplementary Data 6. *P* values calculated using one-way ANOVA with Dunnett's correction. **c**, Optic nerve conduction velocity at 3 weeks of age (*n* = 3 (WT + ASOctr), 8 (*jimpy* + ASOctr) and 4 (*jimpy* + ASO*Plp1*.b) mice). *P* values calculated using one-sided, unpaired *t*-test. **d**, Polynomial trend line illustrating conduction velocity versus brain myelination in *jimpy* + ASO*Plp1*.b to minimum–maximum scaling of values from *jimpy* and wild-type mice treated with ASOctr. Source data from **c** and Fig. 3h with same number of samples. **e**, Trace of a *jimpy* seizure during hypercapnic challenge (*y*-axis, respiratory flow rate). **f**, Minute ventilation (MV) in ml g^{-1} min^{-1} and per gram body weight (ΔMV per g) in 5% CO$_2$ (hypercapnia) and 10.5% O$_2$ (hypoxia),

representing all repeated measurements from *n* = 9 (WT + ASOctr), 6 (*jimpy* + ASOctr) and 7 (*jimpy* + ASO*Plp1*.b) mice. Violin plots indicate median (centre white lines) and quartiles (border white lines). *P* values calculated using Brown and Forsythe's test. **g**–**j**, Minute ventilation per body weight (MV g^{-1}) in normal air (**g**), 15–30 min after transitioning from normal air to 5% CO$_2$ (**h**), 0–3 min (**i**) and 8–9 min (**j**) after transitioning from normal air to 10.5% O$_2$. Post-mortality hypoxia data were not included. In **g**–**i**, *n* = 9 (WT + ASOctr), 6 (*jimpy* + ASOctr) and 7 (*jimpy* + ASO*Plp1*.b) mice; in **j**, *n* = 9 (WT + ASOctr), 3 (*jimpy* + ASOctr) and 7 (*jimpy* + ASO*Plp1*.b) mice. **k**, Kaplan–Meier plot showing survival during hypoxia. *n* = 12 (WT + ASOctr), 8 (*jimpy* + ASOctr) and 9 (*jimpy* + ASO*Plp1*.b) mice. *P* values calculated using log-rank test. Biological replicates (individual mice) indicated by open circles. Data are mean ± s.d., except where indicated. *P* values shown for *P* < 0.1, otherwise not significant.

Further preclinical development is needed to optimize dosage and timing, including treatment later in disease progression; nevertheless, our results highlight that even a single ASO injection can elicit a sustained phenotypic improvement relative to the natural history of the disease, even with restoration of about 10% of myelin relative to wild type. These data could reflect a previously unappreciated functional tolerance to incomplete myelination or may be indicative of a neuronal-supportive function of oligodendrocytes[28–30], levels of which were completely restored in *jimpy* mice injected with *Plp1*-targeting ASOs.

Complete elimination of mutant PLP could convert patients with severe PMD to a *PLP1*-null phenotype, characterized by milder disease

that presents later, progresses slower and shows improved clinical outcomes[1,3–5]. Titration of abnormal or excessive PLP to a level that relieves cellular stress-mediated oligodendrocyte death but maintains the neuronal-supportive function of PLP[3–5,19] could potentially provide greater benefit. This strategy would be especially amendable to the 70% of PMD patients who have gene duplications leading to excess levels of normal PLP protein[1], as a reduction to wild-type levels of PLP expression may be curative.

Collectively, our studies, combined with the feasibility of ASO delivery to the human CNS and current safety data in other CNS indications, support advancement of *PLP1* suppression into the clinic as a

therapeutic strategy with potential applicability across the spectrum of patients with PMD. More broadly, our data provide a framework for transcript modulation in oligodendrocytes to restore myelination in genetic and sporadic disorders of myelination.

Online content

Any methods, additional references, Nature Research reporting summaries, source data, extended data, supplementary information, acknowledgements, peer review information; details of author contributions and competing interests; and statements of data and code availability are available at https://doi.org/10.1038/s41586-020-2494-3.

1. Inoue, K. Pelizaeus–Merzbacher Disease: molecular and cellular pathologies and associated phenotypes. *Adv. Exp. Med. Biol.* **1190**, 201–216 (2019).
2. Wolf, N. I., van Spaendonk, R. M. L., Hobson, G. M. & Kamholz, J. in *Gene Reviews* (eds Adam, M. P. et al.) https://www.ncbi.nlm.nih.gov/books/NBK1182/ (1993).
3. Garbern, J. Y. et al. Patients lacking the major CNS myelin protein, proteolipid protein 1, develop length-dependent axonal degeneration in the absence of demyelination and inflammation. *Brain* **125**, 551–561 (2002).
4. Griffiths, I. et al. Axonal swellings and degeneration in mice lacking the major proteolipid of myelin. *Science* **280**, 1610–1613 (1998).
5. Klugmann, M. et al. Assembly of CNS myelin in the absence of proteolipid protein. *Neuron* **18**, 59–70 (1997).
6. Goldman, S. A., Nedergaard, M. & Windrem, M. S. Glial progenitor cell-based treatment and modeling of neurological disease. *Science* **338**, 491–495 (2012).
7. Gupta, N. et al. Neural stem cell engraftment and myelination in the human brain. *Sci. Transl. Med.* **4**, 155ra137 (2012).
8. Saher, G. et al. Therapy of Pelizaeus–Merzbacher disease in mice by feeding a cholesterol-enriched diet. *Nat. Med.* **18**, 1130–1135 (2012).
9. Wishnew, J. et al. Umbilical cord blood transplantation to treat Pelizaeus–Merzbacher disease in 2 young boys. *Pediatrics* **134**, e1451–e1457 (2014).
10. Tantzer, S., Sperle, K., Kenaley, K., Taube, J. & Hobson, G. M. Morpholino antisense oligomers as a potential therapeutic option for the correction of alternative splicing in PMD, SPG2, and HEMS. *Mol. Ther. Nucleic Acids* **12**, 420–432 (2018).
11. Li, H. et al. Gene suppressing therapy for Pelizaeus–Merzbacher disease using artificial microRNA. *JCI Insight* **4**, 125052 (2019).
12. Nobuta, H. et al. Oligodendrocyte death in Pelizaeus–Merzbacher disease is rescued by iron chelation. *Cell Stem Cell* **25**, 531–541 (2019).
13. Gruenenfelder, F. I. et al. Neural stem cells restore myelin in a demyelinating model of Pelizaeus–Merzbacher disease. *Brain* **143**, 1383–1399 (2020).
14. Elitt, M. S. et al. Chemical screening identifies enhancers of mutant oligodendrocyte survival and unmasks a distinct pathological phase in Pelizaeus–Merzbacher Disease. *Stem Cell Rep.* **11**, 711–726 (2018).
15. Southwood, C. M., Garbern, J., Jiang, W. & Gow, A. The unfolded protein response modulates disease severity in Pelizaeus–Merzbacher disease. *Neuron* **36**, 585–596 (2002).
16. Jinek, M. et al. A programmable dual-RNA-guided DNA endonuclease in adaptive bacterial immunity. *Science* **337**, 816–821 (2012).
17. Cong, L. et al. Multiplex genome engineering using CRISPR/Cas systems. *Science* **339**, 819–823 (2013).
18. Tatar, C. L. et al. Increased *Plp1* gene expression leads to massive microglial cell activation and inflammation throughout the brain. *ASN Neuro* **2**, e00043 (2010).
19. Uschkureit, T., Spörkel, O., Büssow, H. & Stoffel, W. *Rumpshaker*-like proteolipid protein (PLP) ratio in a mouse model with unperturbed structural and functional integrity of the myelin sheath and axons in the central nervous system. *Glia* **35**, 63–71 (2001).
20. Finkel, R. S. et al. Nusinersen versus sham control in infantile-onset spinal muscular atrophy. *N. Engl. J. Med.* **377**, 1723–1732 (2017).
21. Kordasiewicz, H. B. et al. Sustained therapeutic reversal of Huntington's disease by transient repression of huntingtin synthesis. *Neuron* **74**, 1031–1044 (2012).
22. Mazur, C. et al. Brain pharmacology of intrathecal antisense oligonucleotides revealed through multimodal imaging. *JCI Insight* **4**, 129240 (2019).
23. Wu, Q. et al. Elevated levels of the chemokine GRO-1 correlate with elevated oligodendrocyte progenitor proliferation in the *jimpy* mutant. *J. Neurosci.* **20**, 2609–2617 (2000).
24. Miller, M. J. et al. Proteolipid protein gene mutation induces altered ventilatory response to hypoxia in the myelin-deficient rat. *J. Neurosci.* **23**, 2265–2273 (2003).
25. Ueda, A. et al. Pelizaeus–Merzbacher disease can be a differential diagnosis in males presenting with severe neonatal respiratory distress and hypotonia. *Hum. Genome Var.* **5**, 18013 (2018).
26. Osorio, M. J. et al. Concise Review: stem cell-based treatment of Pelizaeus–Merzbacher disease. *Stem Cells* **35**, 311–315 (2017).
27. Renier, W. O. et al. Connatal Pelizaeus-Merzbacher disease with congenital stridor in two maternal cousins. *Acta Neuropathol.* **54**, 11–17 (1981).
28. Lee, Y. et al. Oligodendroglia metabolically support axons and contribute to neurodegeneration. *Nature* **487**, 443–448 (2012).
29. Fünfschilling, U. et al. Glycolytic oligodendrocytes maintain myelin and long-term axonal integrity. *Nature* **485**, 517–521 (2012).
30. Freeman, S. A. et al. Acceleration of conduction velocity linked to clustering of nodal components precedes myelination. *Proc. Natl Acad. Sci. USA* **112**, E321–E328 (2015).

Article

Methods

All data was reproduced with biological replicates as indicated. Blinding was used as indicated. No statistical methods were used to predetermine sample size and the experiments were not randomized. P values shown for $P < 0.1$, otherwise not significant.

Mice

All procedures were in accordance with the National Institutes of Health Guidelines for the Care and Use of Laboratory Animals and were approved by the Case Western Reserve University Institutional Animal Care and Use Committee (IACUC).

Wild-type (B6CBACa-Aw-J/A) and *jimpy* (B6CBACa-Aw-J/A-Plp1jp EdaTa/J; RRID:IMSR_JAX:000287) mice used in this study were purchased from Jackson Laboratory. *jimpy* males possess a point mutation in the splice acceptor site of *Plp1* intron 4 (c.623-2A>G), which results in exclusion of exon 5 and a frameshift of the final 70 amino acids of PLP[31]. The colony was maintained by breeding heterozygous females, which lack a phenotype, to wild-type males to generate affected *jimpy* males. Mice were housed under a temperature-controlled environment, 12 h:12 h light:dark cycle with ad libitum access to water and rodent chow. All mice were genotyped approximately a week after birth using genomic DNA isolated from tail tips or toes at two loci: (1) the *jimpy* mutation (NM_011123.4:c.623-2A>G) in *Plp1* intron 4, which causes skipping of exon 5 and a truncated PLP protein, and (2) the complex indel in *Plp1* exon 3 from dual cutting of CRISPR–Cas9 sgRNAs in CR-*impy* mice (c.[242_318del; 328_330del]). This causes a frameshift in *Plp1*, a premature stop codon in exon 4, and is predicted to cause nonsense-mediated decay of the transcript and loss of protein. Genotyping was performed by standard Sanger sequencing or custom real-time PCR assays (probe identifiers: Plp1-2 Mut [for *jimpy* mutation in intron 4] and Plp1-5 WT [for CR-*impy* complex deletion in exon 3], Transnetyx).

Primers for Sanger sequencing are provided in Supplementary Table 4.

Design of *Plp1*-targeting sgRNA

Mouse *Plp1* sequence was entered into the *Streptococcus pyogenes* CRISPR–spCas9 sgRNA design tool at crispr.mit.edu[32] and analysed against the mm10 target genome. *Plp1*-targeting sgRNAs were sorted on the basis of their on-target efficiency while minimizing off-target mutations. On-target nuclease activity was confirmed for each sgRNA using the Guide-it sgRNA Screening Kit (631440, Clontech) according to the manufacturer's instructions. The following sgRNAs were tested: sgRNA1, CCCCTGTTACCGTTGCGCTC; sgRNA2, TGGCCACCA GGGAAGCAAAG; sgRNA3, AAGACCACCATCTGCGGCAA; sgRNA4, GGCCTGAGCGCAACGGTAAC; sgRNA5, GCCTGAGCGCAACGGTAACA; sgRNA6, TCTACACCACCGGCGCAGTC; sgRNA7, CCAGCAGGAGGGCCC CATAA; and sgRNA8, GAAGGCAATAGACTGACAGG.

This list was further filtered on the basis of the ability of each sgRNA to target *Plp1*'s splice isoform *Dm20*, in addition to *Plp1*. We selected two sgRNAs (3 and 7) that targeted exon 3 of *Plp1* for combined use in zygote studies, which enabled the rapid detection of large deletion events by PCR and provided redundancy for on-target cutting.

Suppression of *Plp1* in *jimpy* zygotes using CRISPR–Cas9

Carrier female oocyte donors were administered 5 IU pregnant mare serum gonadotropin by intraperitoneal injection (G4877, Sigma-Aldrich), followed by 2.5 IU human chorionic gonadotropin (GC10, Sigma-Aldrich) 48 h later. These superovulated females were mated to wild-type males. Zygotes were collected in FHM medium (MR-025 Sigma-Aldrich) with 0.1% hyaluronidase (H3501, Sigma-Aldrich) and the surrounding cumulus cells were separated. The zona pellucida of each zygote was partially dissected using 0.3 M sucrose (S7903, Sigma-Aldrich) in FHM as previously described[33].

Zygotes were placed in 2× KSOM medium (MR-106, Sigma-Aldrich) with an equal volume of solution containing 100 ng μl⁻¹ sgRNA3, 100 ng μl⁻¹ sgRNA7 (AR01, PNAbio), and 200 ng μl⁻¹ spCas9 mRNA (CR01, PNAbio). Given the low frequency of *jimpy* zygotes and unknown in vivo targeting of the sgRNAs, both sgRNAs were used simultaneously to maximize the chance of *Plp1* frameshift. Electroporation was performed in a chamber with a 1-mm gap between two electrodes using an ECM 830 Square Wave Electroporation System (BTX). Electroporation parameters were set as follows: 32 V, 3 ms pulse duration, 5 repeats and 100 ms inter-pulse interval. Electroporated zygotes were moved to KSOM medium and then transferred into the oviducts of pseudo-pregnant females (CD1). Electroporation settings were optimized to achieve maximal cutting efficiency in a separate strain but resulted in a higher rate of embryo loss in our B6CBACa/J strain. Zygotes were electroporated in batches of 54, 56 and 61, which resulted in 4, 3 and 0 pups born. The seven surviving mice were genotyped after birth and monitored daily for onset of typical *jimpy* phenotypes including tremors, seizures and early death by postnatal day 21. A founder *jimpy* male with complex deletion containing 80 bp of total deleted sequence in exon 3 of *Plp1*, denoted CR-*impy*, showed no overt phenotype and was back-crossed for two generations to the wild-type parental strain to reduce potential off-target Cas9 cutting effects (Extended Data Fig. 1b–e). A colony of mice was bred to evaluate cellular, molecular, and functional phenotypes of contemporary isogenic wild-type, *jimpy* and CR-*impy* male mice. Mice were monitored daily to determine lifespan with statistical significance among groups determined using the log-rank test. Additionally, mice surviving beyond three weeks were analysed using behavioural (rotarod and open-field testing for motor performance), histology (immunostaining of the CNS for myelin proteins and electron microscopy for myelin ultrastructure) and electrophysiology (conduction velocity of the optic nerve). Details and metadata for all mice in this study including censoring of animals in the survival analysis are found in Supplementary Data 1.

CRISPR on- and off-target assessment

CRISPR on-target cutting efficiencies were assessed by high-throughput sequencing. PCR primers were designed to encompass each guide on-target site. Primer sequences were generated using NCBI Primer-BLAST and are provided in Supplementary Table 4. The following tails were added to the primer sequences: forward, TCCCT ACACGACGCTCTTCCGATCT; and reverse, AGTTCAGACGTGTGCTCT TCCGATCT.

PCR amplification on tail-tip genomic DNA was performed using the KAPA HiFi HotStart ReadyMix (07958935001, Roche) to minimize PCR-based error. Libraries were prepared by adding unique indices by PCR using KAPA HiFi HotStart ReadyMix. All libraries were pooled evenly and quantified using NEBNext Library Quant Kit for Illumina (E7630, New England Biolabs) then denatured and diluted per Illumina's MiSeq instructions. Then, 250 bp paired-end sequencing was performed using an Illumina MiSeq at the Case Western Reserve University School of Medicine Genomics Core Facility. Reads were compared against the consensus sequence and CRISPR-induced indel percentages were determined using the OutKnocker tool[34] (http://outknocker.org).

Genomic DNA was isolated from brain tissue from the CR-*impy* founder male, three F₂ generation CR-*impy* male mice (each from a unique breeding pair using independent F₁ generation carrier females), and a *jimpy* male from a contemporaneous but independent cohort in our colony. Libraries were prepared for whole genome sequencing using Nextera DNA Flex Library prep (20018705, Illumina) and 150 bp paired-end sequencing was performed using an Illumina NovaSeq. Reads were aligned to the mouse genome (mm10) using BWA[35] (v.0.7.17-r1188) with default parameters for paired reads. Local indel realignment was performed using GATK RealignerTargetCreator and IndelRealigner (v.3.3-2-gec30cee) at the on-target and off-target sites.

Reads aligned to the window chrX:136831817-136832360 at the *Plp1* locus were re-aligned using Blat (v.36x2) to fully capture the CR-*impy* complex deletion.

The top-50 potential off-target sites for each sgRNA were identified using the CCTop - CRISPR–Cas9 target online predictor tool[36], with a maximum total mismatch number of 4. Additionally, each site was identified using the RGEN Cas-OFFinder[37] and CRISPOR[38] off-target prediction algorithms, providing two independent validations of this off-target location list. The indel-realigned reads were visually inspected in Integrative Genomics Viewer (IGV)[39], and indels occurring at a frequency of at least 5% after filtering known polymorphisms from dbSNP (build 142) at these 50 potential off-target sites were considered CRISPR-induced mutations.

Video recording of mouse phenotypes
All recording was performed using video recording function on an Apple iPhone. Videos were colour corrected, stabilized and trimmed to a discrete range using Apple iMovie. Videos were collated and converted to MP4 format using Adobe After Effects.

Immunohistochemistry
Mice were anaesthetized with isoflurane and euthanized by transcardial perfusion with PBS followed by 4% paraformaldehyde (PFA). Tissue was collected and placed in 4% PFA overnight at 4 °C. Samples were rinsed with PBS, equilibrated in 30% sucrose, and frozen in Tissue-Tek Optimum Cutting Temperature compound (OCT; 25608-930, VWR). Samples were cryosectioned at a 20 μm thickness. Sections were washed in phosphate-buffered saline (PBS) and incubated overnight in antibody solution containing 2.5% normal donkey serum (NDS; 017-000-121, Jackson Laboratories) and 0.25% Triton X-100 (T8787, Sigma).

Alternatively, as noted elsewhere in the Methods, mice were euthanized by CO_2 asphyxiation, followed by tissue collection, immersion fixation overnight in 10% neutral-buffered formalin, and paraffin embedding. Sections 5 μm thick were cut onto charged glass slides and dried overnight at 60 °C. Sections were deparaffinized and hydrated using graded concentrations of ethanol to deionized water. Sections were subjected to antigen retrieval by sodium citrate buffer at pH 6 (H-3300; Vector Laboratories) at 100 °C for 45 min, gently washed in deionized water, and then transferred into 0.05 M Tris-based solution in 0.15 M NaCl with 0.1% (v/v) Triton X-100, pH 7.6 (TBST). For chromagen staining, endogenous peroxidase was blocked with 3% hydrogen peroxide for 20 min. Nonspecific background staining was blocked in 3% normal goat serum for 30 min (Sigma) at room temperature. For mouse antibodies, sections were incubated for 30 min in Mouse Blocking Reagent (Vector Laboratories). All slides were then incubated at 4 °C overnight with cocktails of primary antibodies in TBST. For DAB reactions, after washing with TBST, sections were then incubated with the species-appropriate immunoglobulin G (IgG)-horseradish peroxidase (HRP) (1:300, SC2004; Santa Cruz), then reacted with diaminobenzidine (DAB; ScyTek Laboratories) and counterstained with haematoxylin (no. 7211; Richard-Allen Scientific).

Sections were stained using the following antibodies at the indicated concentrations or dilutions: mouse anti-MBP (2 μg ml⁻¹; 808401, Biolegend; RRID:AB_2564741), rabbit anti-MBP (1:1,000; Abcam, ab40390; RRID:AB_1141521), rabbit anti-MyRF polyclonal antibody (1:500; provided by M. Wegner), goat anti-SOX10 (0.4 μg ml⁻¹; AF2864, R&D Systems; RRID:AB_442208), rabbit anti-GFAP (1:1,000; Z0334, Dako; RRID:AB_10013382), goat anti-IBA1 (0.1 mg ml⁻¹; ab5076, Abcam), rabbit anti-IBA1 (1:2,000; 019–19741, WAKO; RRID:AB_839504), rabbit anti-ASO (1:2,500; Ionis Pharmaceuticals), rabbit anti-HDAC2 (1:250; Abcam, ab16032; RRID:AB_2118543), mouse anti-APC/CC1 (2.5 μg ml⁻¹; ab16794, Abcam; RRID:AB_443473), mouse anti-APC/CC1 (1:250; MABC200, Millipore; RRID:AB_11203645), rat anti-NG2 (25 μg ml⁻¹; MAB6689, R&D Systems; RRID:AB_10890940), goat anti-PDGFRα (1:500; AF1062, R&D systems; RRID:AB_2236897) and rabbit anti-OLIG2

(1:250; 13999-1-AP, ProteinTech; RRID:AB_2157541). For MBP immunohistochemistry, sections were post fixed in methanol at -20 °C for 20 min followed by overnight incubation in a PBS based primary antibody solution containing 0.1% saponin and 2.5% normal donkey serum. Secondary immunostaining was performed with Alexa Fluor antibodies (ThermoFisher) used at 1 μg ml⁻¹. Nuclei were identified using DAPI (100 ng ml⁻¹; D8417, Sigma). Stained sections were imaged using the Operetta High Content Imaging and Analysis system (PerkinElmer) and Harmony software (PerkinElmer) for whole-section images and a NanoZoomer S60 Digital slide scanner (Hamamatsu) for all other immunohistochemical imaging, unless otherwise noted.

To quantify MyRF, SOX10, OLIG2, CC1 or PDGFα-positive cells, counts were performed along the length of the whole corpus callosum, the cerebellum and the brainstem in medial sagittal sections from three animals per genotype. CC1 and OLIG2 or PDGFα and OLIG2 double-positive were determined from these counts. Counts were performed in a semi-automated manner using ImageJ (National Institutes of Health). To quantify GFAP and IBA1 staining, fluorescence intensity was measured using Adobe Photoshop along the length of the whole corpus callosum, the cerebellum and the brainstem from medial sagittal sections from three animals per genotype. To quantify cleaved caspase 3 staining, sections from regions starting at the sagittal midline to 600 μm from the midline were used and cleaved caspase 3 positive cells were counted along the entire length of the corpus callosum, white matter of the cerebellum and entire brainstem to determine the total number of apoptotic cells per treatment group. All counts and quantifications were performed in a blinded manner. One-way ANOVA with Tukey's correction and two-way unpaired *t*-tests, or a one-way ANOVA with Dunnett's correction for multiple comparisons were used to determine statistical significance across CRISPR or ASO cohorts, respectively.

RT–qPCR
Mice from CRISPR or ASO studies were euthanized using isoflurane overdose. Different brain regions (cerebral cortex, cerebellum and brainstem) were collected and flash frozen. Each region was split in two and half was used for RNA quantification using RT–qPCR, the other for western blot analysis (see below). TRI Reagent (R2050-1-200, Zymo Research) was separately added to tissue and samples were homogenized using Kontes Pellet Pestle Grinders (KT749520-0000, VWR). RNA was extracted using the RNeasy Mini Kit (74104, Qiagen) according to the manufacturer's instructions. Reverse transcription was performed using the iScript cDNA Synthesis Kit (1708891, Biorad) with 1 μg of RNA per reaction. Real-Time PCR was then performed on an Applied Biosystems 7300 Real-time PCR system with 10 ng cDNA per sample in quadruplicate using Taqman gene expression master mix (4369016, ThermoFisher) and the following pre-designed Taqman gene expression assays (4351370, ThermoFisher): *Plp1* (Mm01297210_m1), *Mbp* (Mm01266402_m1) and *Actb* (Mm00607939_s1) (endogenous control). Expression values were normalized to *Actb* and to wild-type samples (for CRISPR cohort) or wild-type untreated samples (for ASO-treated wild-type cohort). One-way ANOVA with Tukey's correction and two-way unpaired *t*-tests, or a one-way ANOVA with Dunnett's correction for multiple comparisons were used to determine statistical significance across CRISPR or ASO cohorts, respectively.

Protein quantification and western blot
Tissues were obtained as described above. Protein lysis buffer consisting of RIPA buffer (R0278, Sigma), cOmplete Mini EDTA-free Protease Inhibitor Cocktail (11836170001, Sigma), Phosphatase Inhibitor Cocktail 3 (P0044, Sigma), Phosphatase Inhibitor Cocktail 2 (P5726, Sigma), and BGP-15 (B4813, Sigma) was added to each sample. Tissue was homogenized using Dounce Tissue Grinders (D8938, Sigma). Lysate was separated by centrifugation at 17,000g for 15 min at 4 °C. A BCA standard curve was generated using the Pierce BCA Protein Assay Kit (23225, Thermo Scientific) and used to samples to an equivalent

Article

protein concentration. Equal amounts of sample were run on a NuPAGE 4–12% Bis-Tris Protein gel (NP0335BOX or NP0329BOX, Thermo Fisher), then electrophoretically transferred to a PVDF membrane (LC2002, Invitrogen or 926-31097, Li-Cor). The membrane was blocked with 5% milk in TBS-T for an hour, then hybridized with mouse anti-MBP antibody (1 µg ml^{-1}; 808401, Biolegend; RRID:AB_2564741) or rat anti-PLP antibody (1:1,000; clone AA3, Lerner Research Institute Hybridoma Core) overnight at 4 °C. Blots were then washed in TBS-T and incubated in goat anti-mouse HRP (1:2500, 7076, Cell Signaling), goat anti-rat HRP (1:2500, 7077, Cell Signaling) or IRDye secondary antibodies (1:20,000, 925, Li-Cor). Each sample was normalized to β-actin using HRP-conjugated mouse anti-β-actin (1:10,000, A3854, Sigma-Aldrich; RRID:AB_262011). All secondary antibodies were incubated for one hour at room temperature. Blots were analysed with the Odyssey Fc imaging system (Li-Cor). One-way ANOVA with Tukey correction and two-way unpaired t-tests, or a one-way ANOVA with Dunnett's correction for multiple comparisons were used to determine statistical significance across CRISPR or ASO cohorts, respectively. Raw annotated images of full western blots are provided in Supplementary Data 2, 7.

Sample preparation for label-free expression discovery

Samples in protein lysis buffer were cleaned of detergent as described[40], with a 10-kDa molecular weight cutoff filter (Millipore) and buffer exchanged with 8 M urea in 50mM Tris pH 8.0 to a final volume of 50 µl. Proteins were reduced on filter with 10 mM dithiothreitol (8 M urea, 50 mM Tris-pH-8.0) for 1 h at 37 °C, followed by alkylation with 25 mM iodoacetaminde (8 M urea, 50 mM Tris pH 8.0) for 30 min in the dark. The 8 M urea was then adjusted to 4 M (50 mM Tris pH 8.0) and samples were concentrated to a final volume of 50 µl. Next, 10 µg of total protein were digested with lysyl endopeptidase (Wako Chemicals) at an enzyme:substrate ratio of 1:30 for 2 h at 37 °C. The urea concentration was then adjusted to 2 M using 50 mM Tris, pH 8, followed by an overnight trypsin digestion using sequencing grade trypsin (Promega) at an enzyme:substrate ratio of 1:30 at 37 °C.

Reverse phase LC–MS/MS analysis

Three hundred nanograms of each sample were analysed by LC–MS/MS using a LTQ-Orbitrap Elite mass spectrometer (Thermo Scientific) equipped with a nanoAcquity Ultra-high pressure liquid chromatography system (Waters). The injection order on the LC–MS was randomized over all samples. Blank injections were run after each sample to minimize carry-over between samples. Mobile phases were organic phase A (0.1% formic acid in water) and aqueous phase B (0.1% formic acid in acetonitrile). Peptides were loaded onto a nanoACQUITY UPLC 2G-V/M C18 desalting trap column (180 µm × 20 mm nano column, 5 µm, 100 Å) at flow rate of 0.300 µl min^{-1}. Subsequently, peptides were resolved in a nanoACQUITY UPLC BEH300 C18 reversed-phase column (75µm × 250 mm nano column, 1.7 µm, 100 Å; Waters) followed by a gradient elution of 1–40% of phase B over 240 min (isocratic at 1% B, 0–1 min; 2–42% B, 2–212 min; 42–90% B, 212–223 min; and 90–1% B, 223–240 min). A nano ES ion source at a flow rate of 300 nl min^{-1}, 1.5 kV spray voltage and 270 °C capillary temperature was used to ionize peptides. Full scan MS spectra (m/z 380–1,800) were acquired at a resolution of 60,000 followed by twenty data dependent MS/MS scans. LC–MS/MS raw data were acquired using the Xcalibur software (Thermo Fisher Scientific, v.2.2 SP1).

Data processing for protein identification and quantification

The LC–MS/MS raw files (one for each sample) were imported into PeaksStudio (BioinformaticsSolutions) and processed as previously described[41,42]. A database was created that included PLP wild-type and predicted mutant isoforms. Search settings were as follows: trypsin enzyme specificity; mass accuracy window for precursor ion, 10 ppm; mass accuracy window for fragment ions, 0.8 Da; carbamidomethylation of cysteines as fixed modifications; oxidation of methionine as variable modification; and one missed cleavage. Peptide identification

criteria were a mass accuracy of ≤ 10 ppm, and an estimated false discovery rate of less than 2%. Normalization of signal intensities across samples was performed using the average signal intensities obtained in each sample. The fold change was then calculated using these average intensity values for the protein across the two samples.

Electron microscopy

Mice were anaesthetized with isoflurane and tissue was collected after terminal transcardial perfusion with PBS followed by 4% paraformaldehyde and 2% glutaraldehyde (16216, Electron Microscopy Sciences) in 0.1M sodium cacodylate buffer, pH 7.4 (11652, Electron Microscopy Sciences), except for 6-month optic nerve samples which were placed directly into fixative without perfusion. Samples were post-fixed with 1% osmium tetroxide (19150, Electron Microscopy Sciences) and stained with 0.25% uranyl acetate (22400, Electron Microscopy Sciences) en bloc. Samples were dehydrated using increasing concentrations of ethanol, passed through propylene oxide, and embedded in Eponate 12 epoxy resin (18012, Ted Pella). Silver–coloured sections were prepared (Leica EM UC6), placed on 300 mesh nickel grids (T300-Ni, Electron Microscopy Sciences), stained with 2% uranyl acetate in 50% methanol, and stained with lead citrate (17800, Electron Microscopy Sciences). Sections were imaged using a FEI Tecnai Spirit electron microscope at 80 kV. Myelinated axons were manually counted from the sections made on the middle portion of the optic nerve lengthwise, the medial portion of the genu for the corpus collosum, and corticospinal tracts at the pontine level of the brainstem. Three independent areas were counted for each region using Adobe Photoshop (Adobe Systems). Two-way unpaired t-tests or a one-way ANOVA with Dunnett's correction for multiple comparisons were used to determine statistical significance across CRISPR or ASO cohorts, respectively.

Optic nerve electrophysiology

Mice were deeply anaesthetized with isoflurane and euthanized. Each eye with its attached optic nerve was dissected and placed in Tyrode's solution consisting of 129 mM NaCl (BP358-212, Fisher Scientific), 3 mM KCl (BP366-500, Fisher Scientific), 1.2 mM NaH$_2$PO$_4$ (1-3818, J. T. Baker Chemical), 2.4 mM CaCl$_2$ (C79-500, Fisher Scientific), 1.3 mM MgSO$_4$ (M2643, Sigma), 20 mM NaHCO$_3$ (S233-500, Fisher Scientific), 3 mM HEPES (H3375, Sigma), 10 mM glucose (G5767, Sigma), oxygenated using a 95% O$_2$/5% CO$_2$ gas mixture. Each nerve was carefully cleaned, transected behind the eye at the optic chiasm, and allowed to recover for 1 h in oxygenated Tyrode's solution at room temperature (22–24 °C). Each end of the nerve was set in suction electrodes, pulled from polyethylene tubing (PE-190, BD Biosciences). Monophasic electrical stimuli were applied to the proximal end of the nerve and recordings were captured at the distal end. The recovery of the response was monitored every 20 min for 1 h, and only fully recovered samples were subjected to additional stimuli. Stimuli were generated with a S48 stimulator (Grass Technologies) and isolated from ground with PSIU6B unit (Grass Technologies). Supra-threshold stimulus was determined using 30-µs stimulus duration. The response was amplified 100× with a P15D preamplifier (Grass Technologies), monitored with oscilloscope (V1585, Hitachi), digitized with Digidata1550A (Axon Instruments) and recorded using 50-kHz sampling rate with AxoScope software (Axon Instruments). The distance between the electrodes was measured and used to calculate the conduction velocity of the compound action potential peaks at their latency. Recorded signals were analysed using AxoScope software. One-way ANOVA with Tukey correction and two-way unpaired t-tests, or a one-way t-test were used to determine statistical significance across CRISPR or ASO cohorts, respectively.

Open-field testing

Locomotion was assessed by open-field testing. Animals were placed in the centre of a 20-inch by 20-inch square box and all movements were captured for a total of 5 min using ANY-maze software v.5.0

(Stoelting). Total distance travelled was reported for each animal. One-way ANOVA with Tukey correction and two-way unpaired t-tests, or a one-way ANOVA with Dunnett's correction for multiple comparisons were used to determine statistical significance across CRISPR or ASO cohorts, respectively.

Rotarod testing
Motor performance was assessed using a Rota Rod Rotomax 5 (Columbus Instruments) with a 3-cm diameter rotating rod. Immediately before testing, animals were trained at a constant speed of 4 rounds per minute (rpm) for a total of 2 min. Testing began at 4 rpm with an acceleration of $0.1 \, \text{rpm s}^{-1}$. Time to fall was recorded from three independent trials, and the average value for each animal was reported. Animals were allowed to rest for at least 5 min between training and each experimental trial. Animals that failed training were assigned a value of 0 for all three trials for a particular time point. One-way ANOVA with Tukey correction and two-way unpaired t-tests, or a one-way ANOVA with Dunnett's correction for multiple comparisons were used to determine statistical significance across CRISPR or ASO cohorts, respectively.

Immunocytochemistry
Cells were fixed with 4% PFA in PBS. After fixation, cells were permeabilized with 0.2% Triton X-100 in PBS followed by blocking in 10% donkey serum in PBS. Cells were stained overnight at 4 °C with the following primary antibodies diluted in blocking solution: mouse anti-MBP (1:500; 808401, Biolegend; RRID:AB_2564741), rat anti-PLP (1:5,000; clone AA3, Lerner Research Institute Hybridoma Core), goat anti-SOX10 ($2 \, \mu\text{g ml}^{-1}$; AF2864, R&D Systems; RRID:AB_442208), rabbit anti-OLIG2 (1:1,000; 13999-1-AP, ProteinTech; RRID:AB_2157541), rabbit anti-NANOG ($0.4 \, \mu\text{g ml}^{-1}$; AB21624, Abcam; RRID:AB_446437), mouse anti-OCT3/4 ($0.4 \, \mu\text{g ml}^{-1}$; SC-5279, Santa Cruz; RRID:AB_628051). For secondary immunostaining, Alexa Fluor antibodies (ThermoFisher) were used at $1 \, \mu\text{g ml}^{-1}$, and DAPI ($100 \, \text{ng ml}^{-1}$) was used to identify nuclei. Images were captured using Leica DMi8 fluorescence microscope (induced pluripotent stem (iPS) cells) or Operetta High Content Imaging and Analysis system and Harmony software (OPCs and oligodendroctyes), the latter quantified using Columbus software (PerkinElmer).

Generation of iPS cells
Tail tips (2 mm piece from 8-day-old CR-*impy* mice) were bisected, placed on Nunclon-Δ 12-well plates (150628, ThermoFisher), and covered with a circular glass coverslip (12-545-102; Fisher Scientific) to maintain tissue contact with the plate and enable fibroblast outgrowth. Tail-tip fibroblasts were cultured in fibroblast medium consisting of DMEM (11960069, ThermoFisher) with 10% fetal bovine serum (FBS; 16000044, ThermoFisher), 1× non-essential amino acids (11140050, ThermoFisher), 1× Glutamax (35050061, ThermoFisher) and 0.1 mM 2-mercaptoethanol (M3148, SigmaAldrich) supplemented with $100 \, \text{U ml}^{-1}$ penicillin–streptomycin (15070-063, ThermoFisher). Medium was changed every day for the first 3 days and then every other day.

Fibroblasts were seeded at approximately 1.4×10^4 cells per cm^2 on Nunclon-Δ dishes in fibroblast medium, and allowed to equilibrate overnight. The following day, medium was removed and replaced with an equal volume of pHAGE2-TetOminiCMV-STEMCCA-W-loxp lentivirus encoding a floxed, doxycycline-inducible polycistronic Oct4, Sox2, Klf4 and c-Myc construct and pLVX-Tet-On-Puro (632162, Clontech) lentivirus supplemented with $8 \, \mu\text{g ml}^{-1}$ polybrene (107689, Sigma). Lentivirus was prepared using the Lenti-X Packaging Single Shots (631275, Clontech) according to manufacturer's instructions. Three hours later lentivirus medium was removed and replaced with fibroblast medium supplemented with $2 \, \mu\text{g ml}^{-1}$ doxycycline (631311, Clontech). The following day, medium was removed and replaced with an equal volume of pHAGE2-TetOminiCMV-STEMCCA-Wloxp and pLVX-Tet-On-Puro lentivirus supplemented with $8 \, \mu\text{g ml}^{-1}$ polybrene. Three hours later lentivirus medium was diluted 1:2 with fibroblast medium. Medium was

changed each day with fibroblast medium supplemented with $2 \, \mu\text{g ml}^{-1}$ doxycycline and 10^3 units per ml LIF. After 3 days, fibroblasts were lifted using Accutase and seeded on Nunclon-Δ plates, on a feeder layer of irradiated mouse embryonic fibroblasts (iMEFs; produced in-house) previously plated at 1.7×10^4 cells per cm^2 on 0.1% gelatin (1890, Sigma) coated Nunclon-Δ plates in pluripotency medium consisting of Knockout DMEM (10829-018, ThermoFisher), 5% FBS, 15% knockout replacement serum (10828028, ThermoFisher), 1× Glutamax, 1× nonessential amino acids, 0.1 mM 2-mercaptoethanol, and 10^3 units per ml LIF (LIF; ESG1107, EMD Millipore) supplemented with $2 \, \mu\text{g ml}^{-1}$ doxycycline. Medium was changed every day until iPS cell colonies began to emerge. Individual colonies were picked and dissociated in Accutase and were individually plated in single wells of Nunclon-Δ 12-well plates, atop an iMEF feeder layer in pluripotency medium supplemented with 2 $\mu\text{g ml}^{-1}$ doxycycline. Clones were further expanded, with daily medium changes. iPS cell colonies were stained for pluripotency markers Nanog and Oct4 and karyotyped at the seventh passage after derivation (Cell Line Genetics). CR-*impy* iPS cells were derived and characterized for this study (line identifier jpCR100.1). Isogenic comparator *jimpy* (line identifier i.jp-1.6) and wild-type (line identifier i.wt-1.0) iPS cell lines were described and characterized separately[14]. All cell cultures in the laboratory are routinely tested for mycoplasma contamination with consistently negative results. Genotypes of iPS cells were re-verified before use. For characterization iPS cells were immunostained for Nanog and OCT3/4, and counterstained with DAPI.

Generation of iPS-cell-derived OPCs
iPS cells were differentiated to OPCs as previously described[43,44]. In brief, iPS cells were isolated from their iMEF feeder layer using $1.5 \, \text{mg ml}^{-1}$ collagenase type IV (17104019, ThermoFisher) and dissociated with either 0.25% Typsin-EDTA or Accutase and seeded at 7.8×10^4 cells per cm^2 on Costar Ultra-Low attachment 6-well plates (3471, Corning). Cultures were then directed through a stepwise differentiation process to generate pure populations of OPCs. OPCs were maintained in OPC medium consisting of DMEM/F12 (11320082, ThermoFisher), 1× N2 supplement (AR009, R&D Systems), 1× B-27 without vitamin A supplement (12587-010, ThermoFisher), and 1× Glutamax (collectively N2B27 medium), supplemented with $20 \, \text{ng ml}^{-1}$ fibroblast growth factor 2 (FGF2; 233-FB, R&D Systems) and $20 \, \text{ng ml}^{-1}$ platelet-derived growth factor-AA (PDGF-AA; 221-AA, R&D Systems). Medium was changed every other day. All cell cultures in the laboratory are routinely tested for mycoplasma contamination with consistently negative results. For characterization of purity, iPS-cell-derived OPCs were fixed with 4% PFA and immunostained for canonical OPC transcription factors, OLIG2 and SOX10, and counterstained with DAPI.

In vitro assessment of oligodendrocyte differentiation from OPCs
OPCs from each genotype were plated in parallel onto Nunclon-Δ 96-well plates (150628, ThermoFisher) that were first coated with $100 \, \mu\text{g ml}^{-1}$ poly(L-ornithine) (P3655, Sigma), followed by 10 $\mu\text{g ml}^{-1}$ laminin solution (L2020, Sigma). For the oligodendrocyte differentiation assay, 25,000 cells were seeded per well in medium that consisted of DMEM/F12 (11320082, ThermoFisher), 1× N2 supplement (AR009, R&D Systems), 1× B-27 without vitamin A supplement (12587-010, ThermoFisher) and 1× Glutamax, supplemented with T3 ($40 \, \text{ng ml}^{-1}$), Noggin ($100 \, \text{ng ml}^{-1}$), cAMP (10 μM), IGF ($100 \, \text{ng ml}^{-1}$) and NT3 ($10 \, \text{ng ml}^{-1}$). All plates were incubated at 37 °C and 5% CO_2 for 3 days. Cells were fixed and immunostained for MBP and PLP, and counterstained with DAPI. All quantifications were normalized to initial cell counts at plating.

Assessment of gene expression modulation in the oligodendrocyte lineage by *Hdac2*-targeting ASOs
Two ASOs were designed to target mouse *Hdac2*. ASO-*Hdac2*.a consisted of a 20-mer nucleotide sequence (5′-CTCACTTTTCGAGGTTCCTA-3′)

Article

with 2'-O-methoxyethyl modifications and a mixed backbone of phosphorothioate and phosphodiester internucelotide linkages. ASO-*Hdac2*.b consisted of a 16-mer nucleotide sequence (5'-CATCATCTATACCATC-3') with 2'-O-ethyl modifications with a full backbone of phosphorothioate internucelotide linkages. To determine whether ASOs could reduce effectively target oligodendrocyte linage cells and reduce gene expression, we administered *Hdac2*-targeting ASOs to 8-week-old C57BL/6J mice (Jackson Labs) via single 300 µg ICV injection. After 2 weeks, mice were euthanized and processed for histology. Formalin-fixed, paraffin embedded brain and spinal cord sections were stained for NG2 to label OPCs in the study dosed with *Hdac2*.a ASO, and APC/CC1 to oligodendrocytes in the study dosed with *Hdac2*.b ASO, as well for HDAC2 to examine ASO-mediated knockdown of this target. Images were captured using an epifluorescent imaging system (EVOS, ThermoFisher Scientific).

Plp1-targeting ASO design and characterization

Second generation ASOs were designed to target mouse *Plp1*. ASOs consisted of 20-mer nucleotide sequences with 2'-O-methoxyethyl modifications and a mixed backbone of phosphorothioate and phosphodiester internucelotide linkages. ASOs were screened for efficacy in primary E16 cortical cultures, as previously described[45]. In brief, cells were treated with ASOs at 37 °C/5% CO_2 for 3 days, RNA was isolated, and *Plp1* transcript level was quantified with RT–qPCR on Step One instruments (Thermo Fisher). *Plp1* mRNA was normalized to total RNA measured with the Quant-iTTM RiboGreen RNA reagent. ASOs that efficiently reduced *Plpl* mRNA were selected for in vivo screening and tolerability studies.

Lead ASOs were administered to 8-week-old C57BL/6J mice via single 500 µg ICV injection and *Plp1* mRNA levels were measured by RT–qPCR in cortex and spinal cord tissue after 2 weeks. ASOs with greater than 90% *Plp1* mRNA reduction were selected for further characterization. Selected ASOs were administered to mice via single 300 µg ICV bolus injection to test for efficacy and tolerability, as measured by markers of glial cell activation, 8 weeks after ICV injection. Levels of *Plp1* mRNA as well as markers of astrocytes, microglia, and monocytes (*Gfap*, *Aif1* and *Cd68*, respectively) were assessed by RT–qPCR using the custom primer and probe sets (Integrated DNA Technologies) listed in Supplementary Table 4.

Immunohistochemical staining was used to assess morphology of astrocytes, microglia, and oligodendrocyte using anti-GFAP, IBA1 (DAKO), and MBP (Abcam) antibodies, respectively, in formalin-fixed, paraffin embedded brain and spinal cord sections. *Plp1* ASO.a (intron 5) and ASO.b (3' UTR) were selected for use in *jimpy* mice, as well as a control ASO with no known murine target. ASO sequences were as follows: ASO control, 5'-CCTATAGGACTATCCAGGAA-3'; ASO *Plp1*.a, 5'-GCTCATTGATTCAAGTACAT-3'; and ASO *Plp1*.b, 5'-GCATTTACCCGAAGGCCATT-3'.

Each *Plp1*-targeting ASO was further evaluated for potential off-target effects. Bowtie aligner[46] was used to identify putative ASO off-target transcript sequences, with up to three base mismatches. This analysis identified potential off-target sequence in *Xylt1* for ASO *Plp1*.a and *Scfd1* and *Tpk1* for ASO *Plp1*.b, each having exactly two mismatches. To determine whether these transcripts were targeted by *Plp1* ASO.a or ASO.b, adult mice (8 weeks of age, C57Bl6/J) were administered 30, 100 or 300 µg of each ASO by ICV injection. After two weeks, spinal cord tissues were collected and levels of *Xylt1*, *Scfd1* and *Tpk1* were measured by RT–qPCR using the custom primer and probe sets (Integrated DNA Technologies) listed in Supplementary Table 4.

Optimum therapeutic dosage for use in early postnatal injection was determined by injecting wild-type C57BL/6J mice pups at postnatal day 1 using three different doses (10, 30 or 60 µg) of ASO *Plp1*.a or ASO *Plp1*.b, along with a control non-targeting ASO. Mice were euthanized three weeks later and analysed by for levels of *Plp1* mRNA in the spinal cord using RT–qPCR. One-way ANOVA with Dunnett's correction for multiple comparisons was used to determine statistical significance across treatments.

Therapeutic application of ASOs to postnatal mice

Male pups from crosses between *jimpy* mutation carrier females and wild-type males were administered 30 µg of either *Plp1*-targeting ASOs *Plp1*.a, *Plp1*.b, a control non-targeting ASO, or left untreated. ASOs were administered using a Hamilton 1700 gastight syringe (7653-01, Hamilton Company) by ICV injection to cryoanaesthetized mice. The needle was placed between bregma and the eye, 2/5 the distance from bregma, and inserted to a depth of 2 mm (ref. [47]). A total volume of 2 µl was administered to the left ventricle. Mice were allowed to recover on a heating pad and subsequently reintroduced to the dam. Injections were performed with the investigator blinded to the genotype.

Mice were genotyped during the first postnatal week and monitored daily for onset of typical *jimpy* phenotypes including tremors, seizures and early death by 3 weeks of age. Lifespan was determined for each animal with statistical significance among groups determined using the log-rank test. All mice surviving to a pre-determined end point of 8 months of age were euthanized for histological analysis. Additionally, animals were analysed using rotarod, open-field and optic nerve electrophysiology. Details and metadata for all mice in this study are found in Supplementary Data 6.

Evaluation of respiration

At postnatal day 19 or 20, male pups were placed in a plethysmograph chamber and pressure changes caused by animal respiration were measured using a differential pressure transducer (Emka). The data collection was started when the mice were placed in the chamber and continuously recorded at 1 kHz sampling rate. After placing the mice in the chamber, it was first flushed with normal air (79% nitrogen, 21% oxygen) over a 1 h period to acclimatize the mice and determine basal breathing activity. The chamber was then flushed with hypercapnic gas (74% nitrogen, 21% oxygen, 5% carbon dioxide) for 15 min and the data collected over the subsequent 15–30 min period were used for analysis. Next, the chamber was flushed with normal air for 15 min. Hypoxic gas (89.5% nitrogen, 10.5% oxygen) was then introduced to the chamber over 10 min, with the data collected over this period used for analysis. After the hypoxic gas challenge, mice were weighed and euthanized. Gas flow rate over the entire experiment was 0.75 l min^{-1} per chamber. Recorded breaths lasting for at least 20 s, continuously, and marked with a 100% success rate using IOX2 software (Emka) were used for subsequent data analysis for the normal air and hypercapnic conditions. Recorded breaths in the hypoxic condition were not continuous for more than 20 s so only breaths marked with a 100% success rate in the IOX2 software were used for further data analysis. Survival during hypoxic challenge was determined for each animal with statistical significance among groups determined using the log-rank test. Variability of respiration was determined with statistical significance among groups determined using the Brown and Forsythe's test.

Reporting summary

Further information on research design is available in the Nature Research Reporting Summary linked to this paper.

Data availability

All data generated or analysed during this study are included in this article and its Supplementary Information. Animals and iPS cell lines are available from P.J.T. upon request. Source data are provided with this paper.

31. Nave, K. A., Lai, C., Bloom, F. E. & Milner, R. J. Jimpy mutant mouse: a 74-base deletion in the mRNA for myelin proteolipid protein and evidence for a primary defect in RNA splicing. *Proc. Natl Acad. Sci. USA* **83**, 9264–9268 (1986).

32. Hsu, P. D. et al. DNA targeting specificity of RNA-guided Cas9 nucleases. *Nat. Biotechnol.* **31**, 827–832 (2013).

33. Nakagata, N., Okamoto, M., Ueda, O. & Suzuki, H. Positive effect of partial zona-pellucida dissection on the in vitro fertilizing capacity of cryopreserved C57BL/6J transgenic mouse spermatozoa of low motility. *Biol. Reprod.* **57**, 1050–1055 (1997).

34. Schmid-Burgk, J. L. et al. OutKnocker: a web tool for rapid and simple genotyping of designer nuclease edited cell lines. *Genome Res.* **24**, 1719–1723 (2014).

35. Li, H. & Durbin, R. Fast and accurate short read alignment with Burrows–Wheeler transform. *Bioinformatics* **25**, 1754–1760 (2009).

36. Stemmer, M., Thumberger, T., Del Sol Keyer, M., Wittbrodt, J. & Mateo, J. L. CCTop: an intuitive, flexible and reliable CRISPR/Cas9 target prediction tool. *PLoS ONE* **10**, e0124633 (2015).

37. Bae, S., Park, J. & Kim, J. S. Cas-OFFinder: a fast and versatile algorithm that searches for potential off-target sites of Cas9 RNA-guided endonucleases. *Bioinformatics* **30**, 1473–1475 (2014).

38. Haeussler, M. et al. Evaluation of off-target and on-target scoring algorithms and integration into the guide RNA selection tool CRISPOR. *Genome Biol.* **17**, 148 (2016).

39. Robinson, J. T. et al. Integrative genomics viewer. *Nat. Biotechnol.* **29**, 24–26 (2011).

40. Wiśniewski, J. R., Zougman, A., Nagaraj, N. & Mann, M. Universal sample preparation method for proteome analysis. *Nat. Methods* **6**, 359–362 (2009).

41. Tran, N. H. et al. Deep learning enables de novo peptide sequencing from data-independent-acquisition mass spectrometry. *Nat. Methods* **16**, 63–66 (2019).

42. Tran, N. H., Zhang, X., Xin, L., Shan, B. & Li, M. De novo peptide sequencing by deep learning. *Proc. Natl Acad. Sci. USA* **114**, 8247–8252 (2017).

43. Najm, F. J. et al. Rapid and robust generation of functional oligodendrocyte progenitor cells from epiblast stem cells. *Nat. Methods* **8**, 957–962 (2011).

44. Lager, A. M. et al. Rapid functional genetics of the oligodendrocyte lineage using pluripotent stem cells. *Nat. Commun.* **9**, 3708 (2018).

45. Hagemann, T. L. et al. Antisense suppression of glial fibrillary acidic protein as a treatment for Alexander disease. *Ann. Neurol.* **83**, 27–39 (2018).

46. Langmead, B., Trapnell, C., Pop, M. & Salzberg, S. L. Ultrafast and memory-efficient alignment of short DNA sequences to the human genome. *Genome Biol.* **10**, R25 (2009).

47. Glascock, J. J. et al. Delivery of therapeutic agents through intracerebroventricular (ICV) and intravenous (IV) injection in mice. *J. Vis. Exp.* **56**, 2968 (2011).

Author contributions M.S.E. and P.J.T. conceived and managed the overall study. H.E.S and M.S.E. maintained the animal colonies and tracked survival. M.S.E. captured video recordings. L.B. and M.S.E. designed and tested sgRNAs. S.H. performed data analysis for CRISPR off-target assessments. D.F.L., R.A.C. and W.J. performed zygote electroporation and oviduct transfers. H.E.S., B.S.N., K.C.A. and L.B. performed western blot experiments and protein quantification. D.M.S. and H.E.S. performed mass spectrometry sample preparation and analysis. B.E.P., L.B., B.S.N. and K.C.A. performed RT–qPCR. M.M., B.S.N, L.B., H.E.S., A.S.G. and M.S.E. generated and quantified the immunohistochemistry data. Y.M.-H. performed optic nerve electrophysiology studies and analysed the data. Y.M.-H., M.H., M.S.E. and H.E.S. processed samples for electron microscopy. Y.M.-H. analysed and quantified electron microscopy images. M.S.E., K.C.A., B.S.N. and L.B. performed rotarod and open-field experiments. M.S.E., B.S.N., K.C.A. and H.E.O. generated and characterized iPS cells and OPCs in vitro. H.T.Z. and A.S. generated *Hdac2*-targeting ASO data. B.E.P. and F.R. designed and characterized *Plp1*-targeting ASOs, tested tolerability in adult mice, recommended the use of ASOs, and contributed to the study design and interpretation of results in the ASO-treated disease model. M.S.E. performed ASO injections in *jimpy* mice. Y.M.-H. and B.S.N. performed all respiratory evaluations and analysed the data. Z.S.N. contributed key components to experimental design, data analysis and manuscript composition. M.S.E. and L.B. performed statistical analyses. M.S.E., M.M., Y.M.-H., L.B. and P.J.T. assembled figures. M.S.E. and P.J.T. wrote the manuscript with input from all authors.

Competing interests P.J.T. and M.S.E. are listed as inventors on pending patent claims (PCT/US2017/064870) filed by CWRU covering methods of PLP1 suppression. P.J.T. is a co-founder and consultant for Convelo Therapeutics, which has licensed patents unrelated to the current study from CWRU inventors (P.J.T., M.S.E., Z.S.N. and M.M.). P.J.T. and CWRU retain equity in Convelo Therapeutics. P.J.T. is a consultant and on the Scientific Advisory Board of Cell Line Genetics, which performed karyotyping in this study. P.J.T. is Chair of the Scientific Advisory Board (volunteer position) for the Pelizaeus-Merzbacher Disease Foundation. B.E.P., H.T.Z., A.S. and F.R. are employees of Ionis Pharmaceuticals. No other authors declare competing interests.

Additional information
Supplementary information is available for this paper at https://doi.org/10.1038/s41586-020-2494-3.
Correspondence and requests for materials should be addressed to P.J.T.
Peer review information *Nature* thanks Evan Goldstein and the other, anonymous, reviewer(s) for their contribution to the peer review of this work.
**Reprints and permissions information** is available at http://www.nature.com/reprints.

Extended Data Fig. 1 | See next page for caption.

Extended Data Fig. 1 | CRISPR nuclease induction of *Plp1* frameshift mutations in *jimpy* with high accuracy. a, Annotated Sanger sequencing traces of wild-type, *jimpy*, and CR-*impy* mice showing the complex, frameshift in *Plp1* exon 3 from dual cutting of CRISPR/spCas9 sgRNAs in CR-*impy* mice as well as the *jimpy* point mutation in intron 4. sgRNA 3 and 7 sequences outlined by black boxes with the predicted double strand break site shown a black arrow. **b**, Table showing the top predicted on- and off-target sites for sgRNAs 3 and 7. CRISPR-induced indels were detected by whole genome sequencing of the CR-*impy* founder and three independent CR-*impy* F2 generation males, and consisted of an on-target 80bp complex deletion (CR-*impy* deletion) in exon 3 of *Plp1* (green), an off-target 1 bp insertion in chromosome 6 (red), and an off-target 1 bp insertion in chromosome 11 (yellow). **c**–**e**, Integrative Genomics Viewer browser images showing aligned reads for the CR-*impy* founder, the *jimpy* control, and three CR-*impy* F2 males along with the detected indels at the on-target locus at exon 3 of *Plp1* on chromosome X (**c**), and off-targets on chromosome 6 (**d**) and chromosome 11 (**e**) depicted by the dashed green, red, and yellow boxes, respectively. sgRNA 3 or sgRNA 7 targeted sequences are depicted by black bars.
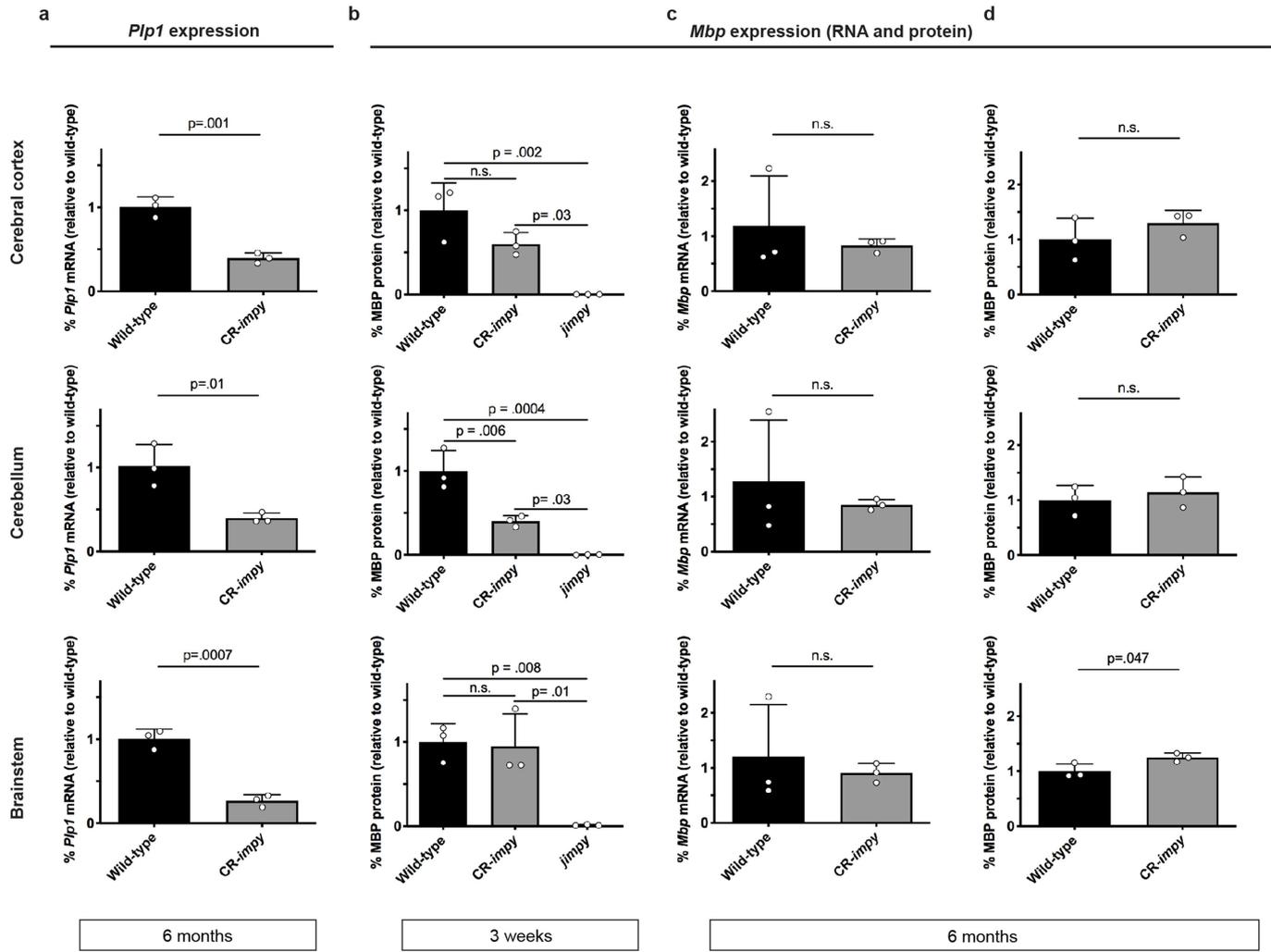
Extended Data Fig. 2 | CRISPR-mediated suppression of *Plp1* in *jimpy* mice increases *Mbp* expression across multiple CNS regions. a, RT–qPCR data showing the levels of *Plp1* transcript at 6 months (*n* = 3 mice). **b**, western blot data demonstrating the levels of MBP protein at 3 weeks (*n* = 3 mice). **c**, RT–qPCR data showing the levels of *Mbp* transcript at 6 months (*n* = 3 mice). **d**, western blot data demonstrating the levels of MBP protein at 6 months (*n* = 3 mice). Individual data points represent the mean value of 4 technical replicates for each biological replicate (**a**, **c**) or independent biological replicates (**b**, **d**). Biological replicates (individual mice) indicated by open circles. Graph bars indicate mean ± standard deviation. p-values calculated using one-way ANOVA with Tukey correction at 3 weeks or two-way, an unpaired two-sided *t*-test at later time points. p-values stated for *P* < 0.1, otherwise not significant (n.s). See Supplementary Data 2 for full western blot images for all samples.
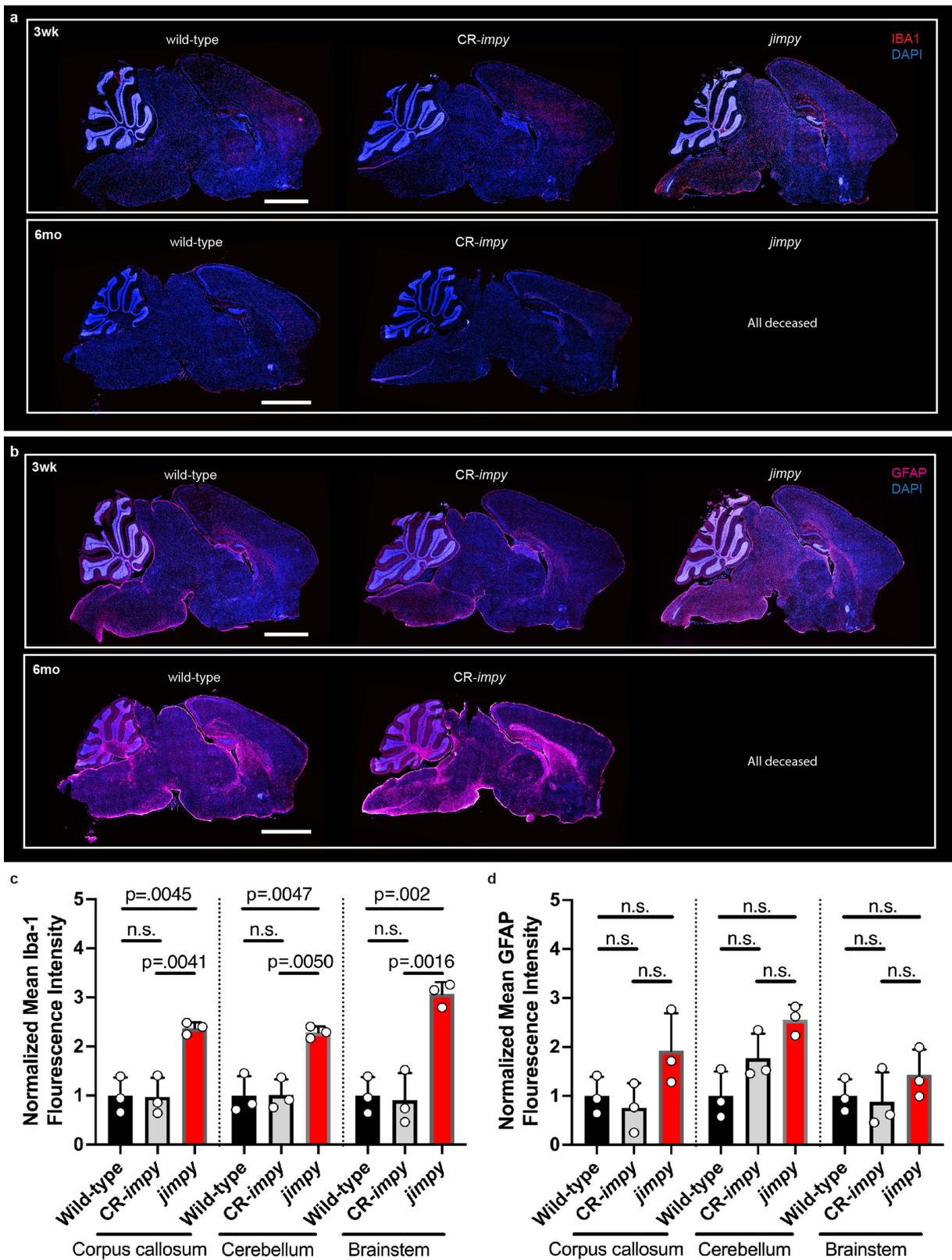
Extended Data Fig. 3 | CRISPR-mediated suppression of *Plp1* in *jimpy* mice reduces markers of activated microglia and astrocytes. a, Immunohistochemical images of whole-brain sagittal sections showing Iba1+ microglia (red) and DAPI+ nuclei (blue) across genotypes. Scale bar, 2mm. **b,** Immunohistochemical images of whole-brain sagittal sections showing GFAP+ astrocytes (red) and DAPI+ nuclei (blue) staining across genotypes. Scale bar, 2mm. **c, d,** Normalized mean signal intensity of (**c**) Iba1+ microglia and (**d**) GFAP+ astrocytes across genotypes and CNS regions (*n* = 3 mice). Biological replicates (individual mice) indicated by open circles. Graph bars indicate mean ± standard deviation. p-values calculated using one-way ANOVA with Tukey correction. p-values stated for *P* < 0.1, otherwise not significant (n.s). See Supplementary Data 3-5 for representative source images of Iba-1 and GFAP staining.
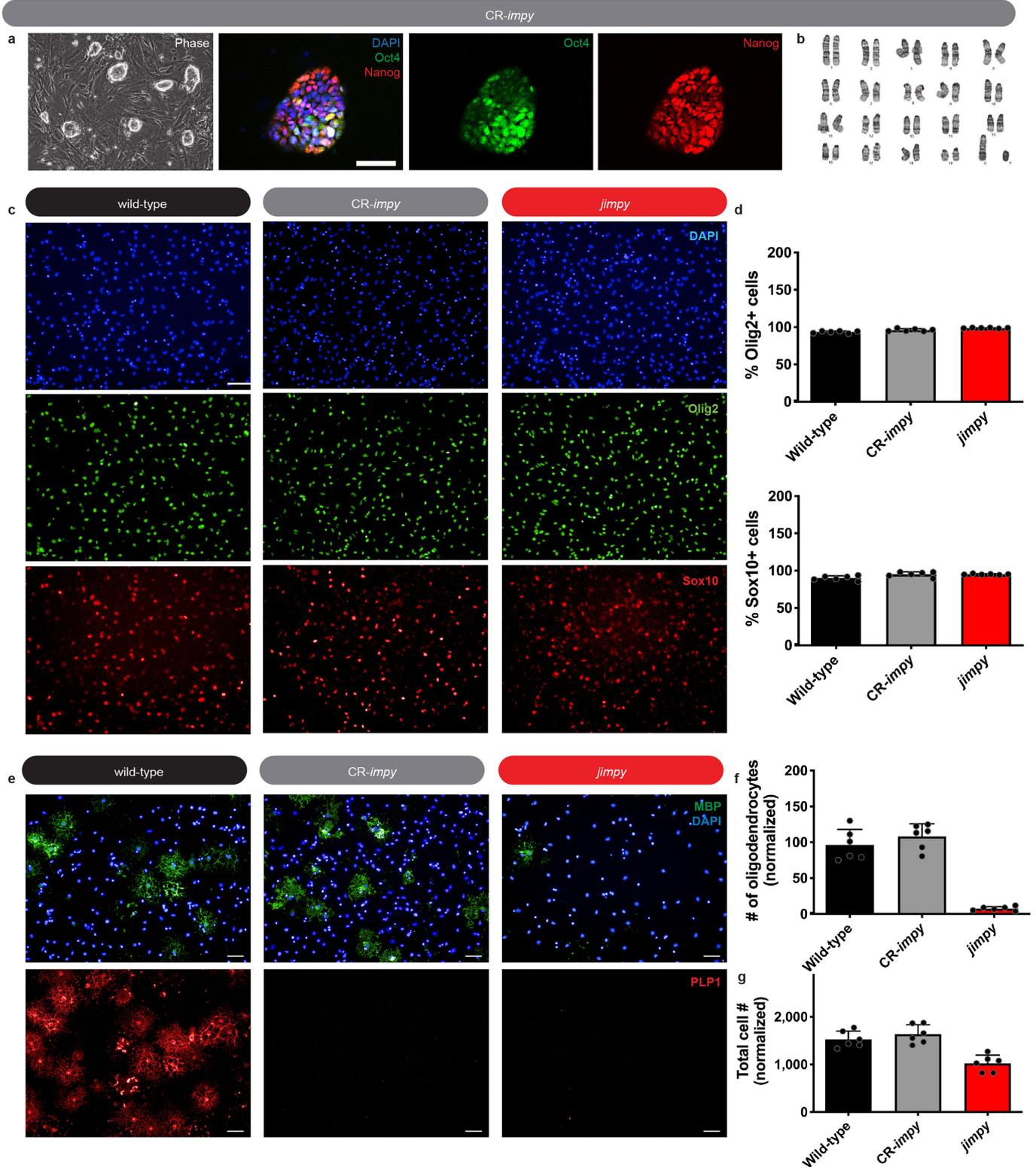
Extended Data Fig. 4 | *Plp1* suppression in *jimpy* OPCs rescues survival of differentiating oligodendrocytes in vitro. a, Phase and immunocytochemistry images of Oct4+ and Nanog+ iPS cells, along with DAPI+ nuclei and **b**, normal karyotype of a CR-*impy* iPS cell line used to generate OPCs. Scale bar, 50μm. **c**, Immunocytochemistry images showing Olig2+ and Sox10+ cells in OPC cultures, along with DAPI+ nuclei, derived from iPS cells. Scale bar, 100μm. **d**, Percentage of Sox10+ and Olig2+ cells in OPC cultures. **e**, Immunocytochemistry images of MBP+ and PLP+ oligodendrocytes. **f**, **g**, Quantification of (**f**) MBP+ oligodendrocytes and (**g**) total cell number (DAPI+ nuclei) from iPS-cell-derived OPCs differentiated in vitro for 3 days. Scale bar, 50μm. Technical replicates (individual wells) for a single cell line per genotype indicated by black circles. Graph bars indicate mean ± standard deviation.
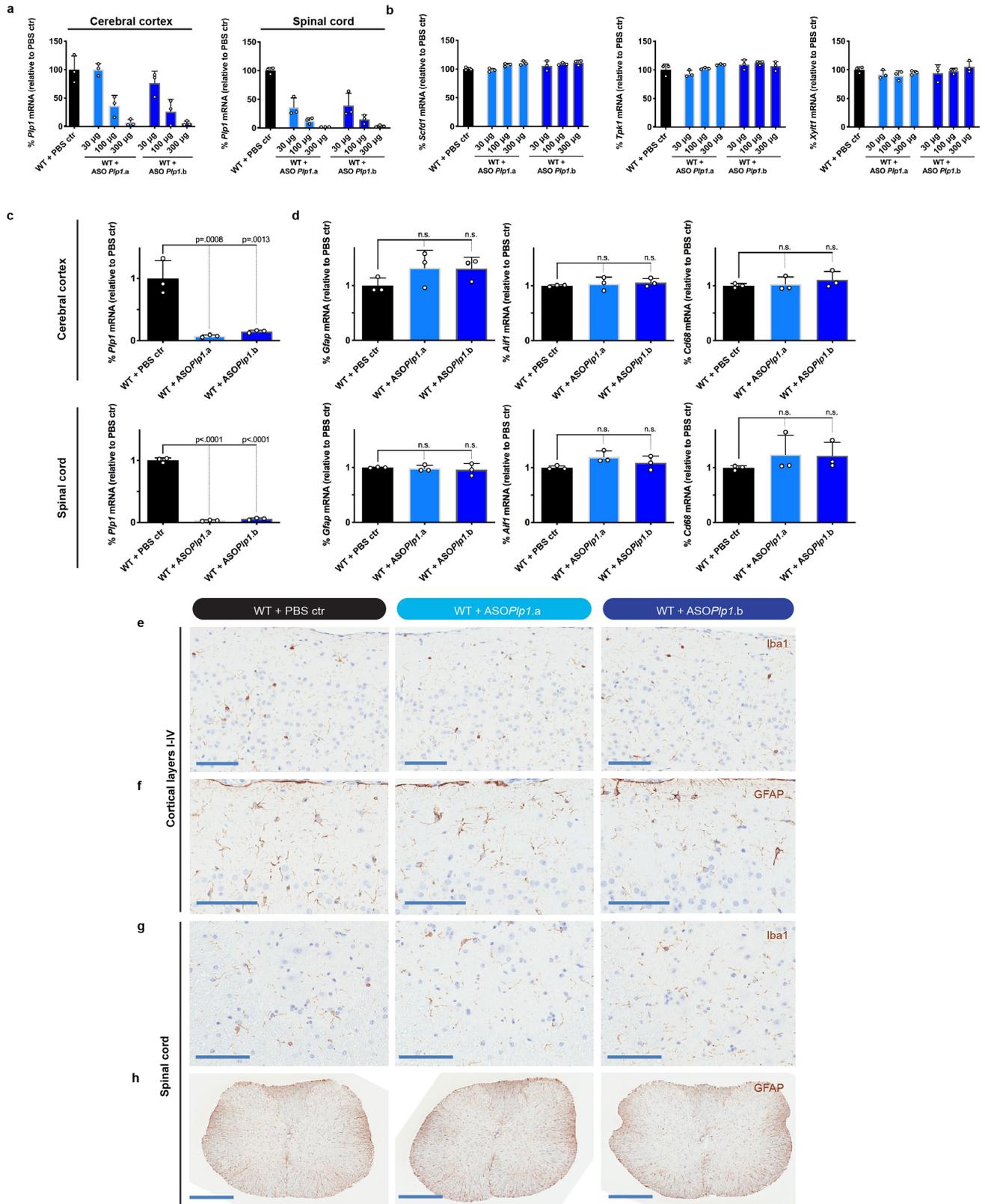
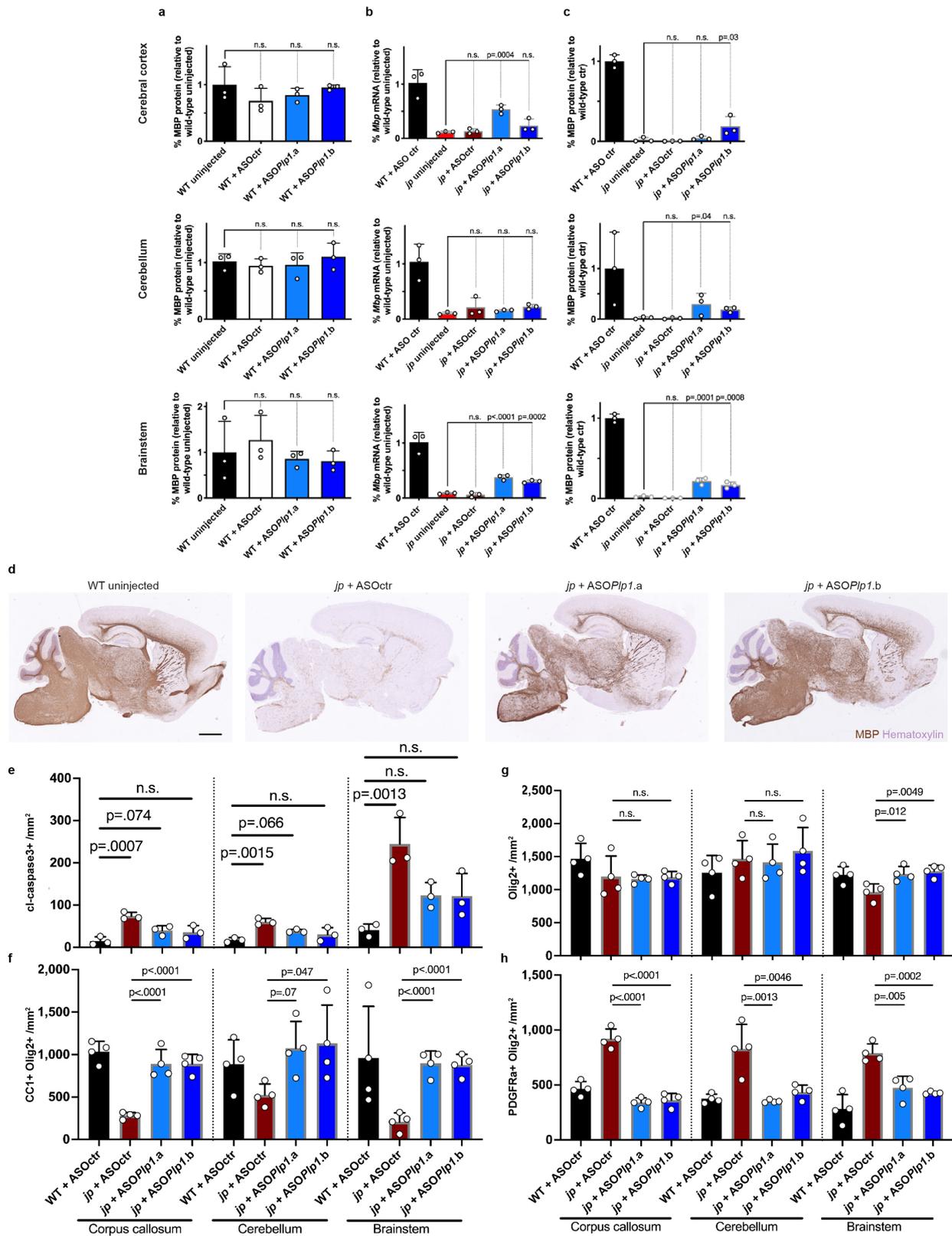**Extended Data Fig. 5** | See next page for caption.

Article

Extended Data Fig. 5 | *Plp1*-targeted ASOs do not suppress off-target transcripts or activate glial cells. a, **b**, RT–qPCR data showing the level of (**a**) *Plp1* transcript levels or (**b**) expression levels of off-target transcripts (up to 3 base mismatches) in the spinal cord for *Plp1*-tageting ASOs, including *Xylt1* (off-target for ASO *Plp1*.a), *Scfd1*, or *Tpk1* (off-targets for ASO *Plp1*.b), 2 weeks post-injection of *Plp1*-targeting ASOs (30µg, 100µg, and 300µg doses) or PBS control in 8 week old adult wild-type (wt) mice ($n = 3$ mice). **c**, **d**, RT–qPCR data showing *Plp1* transcript levels or tolerability by expression levels of *Gfap, Aif1*, and *Cd68* transcripts in the cerebral cortex and spinal cord, 8 weeks post-injection with the indicated ASOs (300µg dose) or PBS control in 8 week old wild-type mice ($n = 3$ mice). **e**–**h**, Immunohistochemistry images with haematoxylin counterstain showing Iba1+ or GFAP+ astrocytes in **e**, Cortical layers I-IV (Iba1), (**f**) cortical layers I-III (GFAP), (**g**) spinal cord dorsal horn grey/white matter intersection (Iba1), and (**h**) spinal cord (GFAP), 8 weeks post-injection with the indicated ASOs (300µg dose) or PBS control in 8 week old wild-type mice. Scale bar, 500µm. Biological replicates (individual mice) indicated by open circles, representing the mean value of 3 technical replicates. Graph bars indicate mean ± standard deviation. p-values calculated using one-way ANOVA with Dunnett's correction for multiple comparisons. p-values stated for $P < 0.1$, otherwise not significant (n.s).
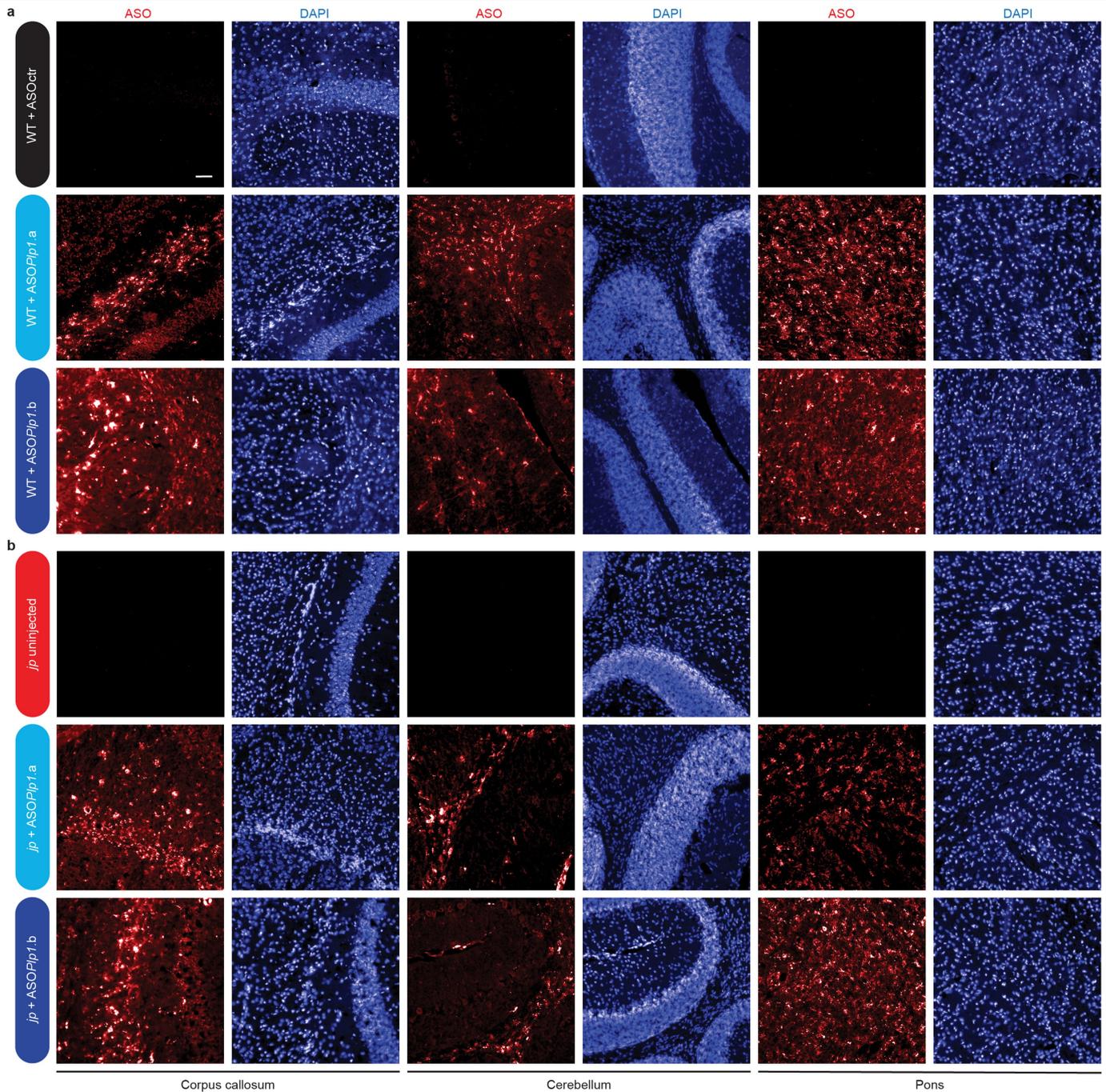
Extended Data Fig. 6 | *Plp1*-targeted ASOs distribute widely throughout the CNS after ICV injection in postnatal mice. a, **b**, Immunohistochemical images of brain sagittal sections showing ASO⁺ staining and DAPI⁺ nuclei (blue) of WT + ASO*Plp1.a*, WT + ASO*Plp1.b* and WT uninjected (**a**) or jp + ASO*Plp1.a*, jp + ASO*Plp1.b* and *jimpy* uninjected mice (**b**), 3 weeks post-ASO injection (30 μg dose at birth). Scale bar, 50 μm.

Extended Data Fig. 7 | See next page for caption.

Extended Data Fig. 7 | *Plp1*-targeting ASOs increase *Mbp* expression and rescue oligodendrocyte numbers in *jimpy* mice. a, Western blot data showing the level of MBP protein (*n* = 3 mice). **b**, RT–qPCR data showing the level of *Mbp* transcript (*n* = 3 mice). **c**, Western blot data showing the level of MBP (*n* = 3 mice). **d**, Immunohistochemistry images with haematoxylin counterstain of whole brain sagittal sections showing MBP⁺ myelin. Scale bar, 1mm. **e**, Quantification of cleaved-caspase 3⁺ apoptotic cells (*n* = 3 mice). **f**, Quantification of CC1⁺/Olig2⁺ oligodendrocytes (*n* = 4 mice). **g**, Quantification of the number of Olig2⁺ glial lineage cells (*n* = 4 mice). **h**, Quantification of the number of PDGFRα⁺/Olig2⁺ OPCs (*n* = 4 mice). All data collected at 3 weeks post-ASO injection (30µg dose at birth). Individual data points represent the mean value of 4 technical replicates for each biological replicate (individual mice) (**b**) or independent biological replicates (individual mice) (**a**, **c**–**h**), indicated by open circles. Graph bars indicate mean ± standard deviation. p-values calculated using one-way ANOVA with Dunnett's correction for multiple comparisons. p-values stated for *P* < 0.1, otherwise not significant (n.s). See Supplementary Data 4 for full western blot images for all samples.
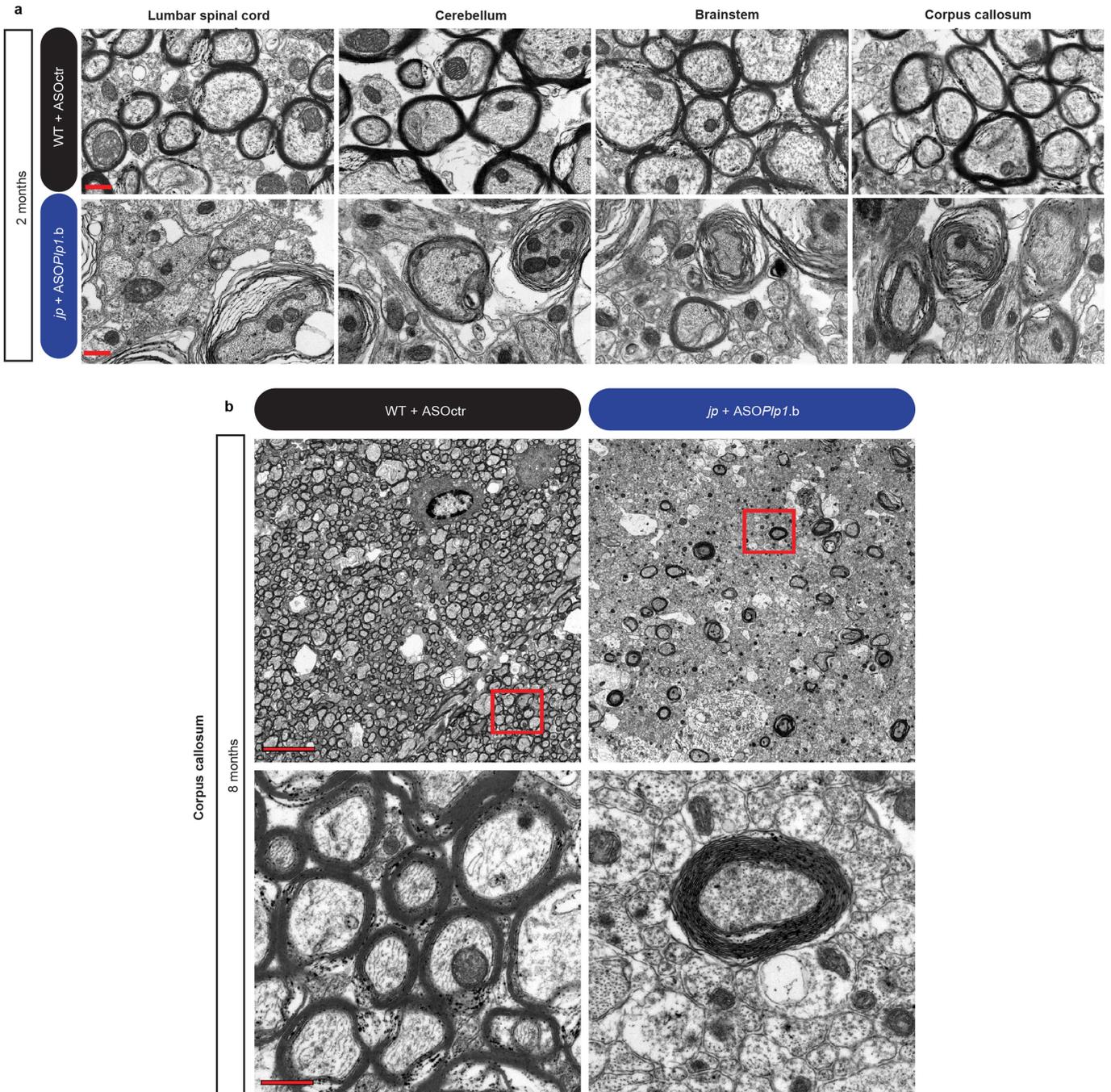
Extended Data Fig. 8 | *Plp1*-targeted ASOs induce sustained myelination throughout the neuraxis in *jimpy* mice. a, b, Electron micrograph images showing myelination of WT + ASOctr or *jp* + ASO*Plp1.b* at 2 months (**a**) and 8 months (**b**). For **a**, scale bar, 0.5 μm. In **b**, the bottom panel is a higher magnification of red boxed area in the top panel. Scale bars, 5 μm (top) and 0.5 μm (bottom).

nature research

Corresponding author(s):	Paul J. Tesar
Last updated by author(s):	Jun 6, 2020

Reporting Summary

Nature Research wishes to improve the reproducibility of the work that we publish. This form provides structure for consistency and transparency in reporting. For further information on Nature Research policies, see Authors & Referees and the Editorial Policy Checklist.

Statistics

For all statistical analyses, confirm that the following items are present in the figure legend, table legend, main text, or Methods section.

n/a	Confirmed	
☐	☒	The exact sample size (*n*) for each experimental group/condition, given as a discrete number and unit of measurement
☐	☒	A statement on whether measurements were taken from distinct samples or whether the same sample was measured repeatedly
☐	☒	The statistical test(s) used AND whether they are one- or two-sided *Only common tests should be described solely by name; describe more complex techniques in the Methods section.*
☒	☐	A description of all covariates tested
☐	☒	A description of any assumptions or corrections, such as tests of normality and adjustment for multiple comparisons
☐	☒	A full description of the statistical parameters including central tendency (e.g. means) or other basic estimates (e.g. regression coefficient) AND variation (e.g. standard deviation) or associated estimates of uncertainty (e.g. confidence intervals)
☐	☒	For null hypothesis testing, the test statistic (e.g. *F*, *t*, *r*) with confidence intervals, effect sizes, degrees of freedom and *P* value noted *Give P values as exact values whenever suitable.*
☒	☐	For Bayesian analysis, information on the choice of priors and Markov chain Monte Carlo settings
☒	☐	For hierarchical and complex designs, identification of the appropriate level for tests and full reporting of outcomes
☒	☐	Estimates of effect sizes (e.g. Cohen's *d*, Pearson's *r*), indicating how they were calculated

Our web collection on statistics for biologists contains articles on many of the points above.

Software and code

Policy information about availability of computer code

Data collection	Images were acquired with Leica Application Suite X, Hamamatsu NDP 2.0, or Perkin Elmer Operetta Harmony software. Videos were acquired using an Apple iPhone. Optic nerve conduction velocity was recorded using AxoScope software(Molecular Devices). Behavioral measurements were recorded using ANY-maze software version 5.0 (open field) and Rota Rod Rotomax 5 (rotarod). Breathing was recorded on the IOX2 software (Emka).
Data analysis	Graphpad Prism was used to generate graphs and perform statistics. Adobe Photoshop, NIH ImageJ, and Perkin Elmer Harmony and Columbus software were used for calculations and cell counting. spCas9 CRISPR sgRNA design tool at crispr.mit.edu was used to design sgRNAs. CRISPR-induced indels were analyzed using the OutKnocker tool at outknocker.org, GATK RealignerTargetCreator, IndelRealigner (version 3.3-2-gec30cee), Blat (v. 36x2), CCTop, RGEN Cas-OFFinder, CRISPOR, and the Integrative Genomics Viewer. Bowtie aligner 58 was used to identify putative ASO off-target transcript sequences. Adobe Photoshop and Illustrator were used to assemble images. Blots were analyzed with the Odyssey Fc imaging system (Li-Cor). LC-MS/MS data was analyzed using BioinformaticsSolutions PeaksStudio software.

For manuscripts utilizing custom algorithms or software that are central to the research but not yet described in published literature, software must be made available to editors/reviewers. We strongly encourage code deposition in a community repository (e.g. GitHub). See the Nature Research guidelines for submitting code & software for further information.

Data

Policy information about availability of data

All manuscripts must include a data availability statement. This statement should provide the following information, where applicable:

- Accession codes, unique identifiers, or web links for publicly available datasets
- A list of figures that have associated raw data
- A description of any restrictions on data availability

All data generated or analyzed during this study are included in this article and its supplementary information files. Source data for animal survival cohorts in Figs. 1b, k-l, and 3b, 4a-b are provided in Supplementary Data 1 and 6. Raw annotated western blot images for Extended Data Fig. 2b, d and Extended Data Fig. 7a, c are

provided as Supplementary Data 2 and 7. Source data for all graphs are provided as separate Excel files. Animals and iPSC lines are available from P.J.T. upon request.

Field-specific reporting

Please select the one below that is the best fit for your research. If you are not sure, read the appropriate sections before making your selection.

☒ Life sciences ☐ Behavioural & social sciences ☐ Ecological, evolutionary & environmental sciences

For a reference copy of the document with all sections, see nature.com/documents/nr-reporting-summary-flat.pdf

Life sciences study design

All studies must disclose on these points even when the disclosure is negative.

Sample size	No statistical test was used to predetermine sample size. Instead, sample sizes were rationalized by considering sufficient replication (weighing the level of biological variation) as well as censoring (due to tissue harvesting at pre-determined time-points and inadvertent losses).
Data exclusions	All data points were included in analyses except for certain animals that were censored from survival analyses to use in pre-determined terminal assays. Metadata for all mice in this study including censoring of animals in the survival analyses are found in Supplementary Figs. 1 and 3.
Replication	The ASO therapeutic response was tested with two independent ASOs and all data were replicated.
Randomization	Sample allocation was not random. Instead, biological controls were employed in all experiments.
Blinding	Investigators were blinded to animal genotype at the time of ASO injection. Investigators were blinded to genotype and treatment for immunohistochemistry quantifications. For other experiments (i.e. animal behavior, electrophysiology, and respiratory analysis) blinding was not possible due to the overt jimpy phenotype.

Reporting for specific materials, systems and methods

We require information from authors about some types of materials, experimental systems and methods used in many studies. Here, indicate whether each material, system or method listed is relevant to your study. If you are not sure if a list item applies to your research, read the appropriate section before selecting a response.

Materials & experimental systems

n/a	Involved in the study
☐	☒ Antibodies
☐	☒ Eukaryotic cell lines
☒	☐ Palaeontology
☐	☒ Animals and other organisms
☒	☐ Human research participants
☒	☐ Clinical data

Methods

n/a	Involved in the study
☒	☐ ChIP-seq
☒	☐ Flow cytometry
☒	☐ MRI-based neuroimaging

Antibodies

Antibodies used	Primary antibodies used for IHC: mouse anti-MBP (2µg/mL; 808401, Biolegend; RRID:AB_2564741), rabbit anti-MBP (1:1000; Abcam, ab40390; RRID:AB_1141521), rabbit anti-MyRF polyclonal antibody (1:500; kindly provided by Dr. Michael Wegner), goat anti-SOX10 (0.4µg/mL; AF2864, R&D Systems; RRID:AB_442208), rabbit anti-GFAP (1:1000; Z0334, Dako; RRID:AB_10013382), goat anti-IBA1 (0.1mg/mL; ab5076, Abcam), rabbit anti-IBA1 (1:2000; 019–19741, WAKO; RRID:AB_839504), rabbit anti-ASO (1:2500; Ionis Pharmaceuticals, Carlsbad, CA), rabbit anti-HDAC2 (1:250; Abcam, ab16032; RRID:AB_2118543), mouse anti-APC/CC1 (2.5 µg/ml; ab16794, Abcam; RRID:AB_443473), mouse anti-APC/CC1 (1:250; MABC200, Millipore; RRID:AB_11203645), rat anti-NG2 (25 µg/mL; MAB6689, R&D Systems; RRID:AB_10890940), goat anti-PDGFRα (1:500; AF1062, R&D systems; RRID:AB_2236897), and rabbit anti-OLIG2 (1:250; 13999-1-AP, ProteinTech; RRID:AB_2157541). Primary antibodies used for western blot: mouse anti-MBP antibody (1µg/mL; 808401, Biolegend; RRID:AB_2564741) and rat anti-PLP antibody (1:1000; clone AA3, Lerner Research Institute Hybridoma Core, Cleveland, OH). Primary antibodies used for ICC: mouse anti-MBP (1:500; 808401, Biolegend; RRID:AB_2564741), rat anti-PLP (1:5000; clone AA3, Lerner Research Institute Hybridoma Core, Cleveland, OH), goat anti-SOX10 (2µg/mL; AF2864, R&D Systems; RRID:AB_442208), rabbit anti-OLIG2 (1:1000; 13999-1-AP, ProteinTech; RRID:AB_2157541), rabbit anti-NANOG (0.4µg/mL; AB21624, Abcam; RRID:AB_446437), mouse anti-OCT3/4 (0.4µg/mL; SC-5279, Santa Cruz; RRID:AB_628051).

Validation	Primary antibodies used in this study are well accepted in the field and purchased from reputable suppliers with provided quality control metrics.

Eukaryotic cell lines

Policy information about cell lines

Cell line source(s)	Mouse iPSC lines were generated in-house
Authentication	Cells lines were genotyped, karotyped, and stained for canonical markers of OPCs and iPSCs.
Mycoplasma contamination	Laboratory cell lines are routinely tested for mycoplasma contamination with consistently negative results.
Commonly misidentified lines (See ICLAC register)	No commonly misidentified cell lines were used in this study.

Animals and other organisms

Policy information about studies involving animals; ARRIVE guidelines recommended for reporting animal research

Laboratory animals	Male jimpy mice (B6CBACa-Aw-J/A-Plp1jp EdaTa/J; RRID:IMSR_JAX:000287), CRISPR modified jimpy (CR-impy) mice (this paper) and wild-type controls. All mice were on a B6CBACa background.
Wild animals	No wild animals were used in this study.
Field-collected samples	No field-collected samples were used in this study.
Ethics oversight	All procedures were in accordance with the National Institutes of Health Guidelines for the Care and Use of Laboratory Animals and were approved by the Case Western Reserve University Institutional Animal Care and Use Committee (IACUC).

Note that full information on the approval of the study protocol must also be provided in the manuscript.